

HYDRATION BEHAVIOR AND STRENGTH DEVELOPMENT OF  
MINERAL ADMIXTURE INCORPORATED CALCIUM ALUMINATE  
CEMENTS

A THESIS SUBMITTED TO  
THE GRADUATE SCHOOL OF NATURAL AND APPLIED SCIENCES  
OF  
MIDDLE EAST TECHNICAL UNIVERSITY

BY

KADİR CAN ERKMEN

IN PARTIAL FULFILLMENT OF THE REQUIREMENTS  
FOR  
THE DEGREE OF MASTER OF SCIENCE  
IN  
CIVIL ENGINEERING

OCTOBER 2018



Approval of the thesis:

**HYDRATION BEHAVIOR AND STRENGTH DEVELOPMENT OF  
MINERAL ADMIXTURE INCORPORATED CALCIUM ALUMINATE  
CEMENTS**

submitted by **KADİR CAN ERKMEN** in partial fulfillment of the requirements  
for the degree of **Master of Science in Civil Engineering Department, Middle  
East Technical University** by,

Prof. Dr. Halil Kalıpçılar  
Dean, Graduate School of **Natural and Applied Sciences** \_\_\_\_\_

Prof. Dr. İsmail Özgür Yaman  
Head of Department, **Civil Engineering** \_\_\_\_\_

Prof. Dr. Mustafa Tokyay  
Supervisor, **Civil Engineering Dept., METU** \_\_\_\_\_

**Examining Committee Members:**

Prof. Dr. İsmail Özgür Yaman  
Civil Engineering Dept., METU \_\_\_\_\_

Prof. Dr. Mustafa Tokyay  
Civil Engineering Dept., METU \_\_\_\_\_

Prof. Dr. Sinan Turhan Erdoğan  
Civil Engineering Dept., METU \_\_\_\_\_

Asst. Prof. Dr. Çağla Meral Akgül  
Civil Engineering Dept., METU \_\_\_\_\_

Asst. Prof. Dr. Seda Yeşilmen  
Civil Engineering Dept., Çankaya University \_\_\_\_\_

**Date:** \_\_\_\_\_ 30.10.2018 \_\_\_\_\_

**I hereby declare that all information in this document has been obtained and presented in accordance with academic rules and ethical conduct. I also declare that, as required by these rules and conduct, I have fully cited and referenced all material and results that are not original to this work.**

Name, Last name: Kadir Can Erkmen

Signature:

## **ABSTRACT**

### **HYDRATION BEHAVIOR AND STRENGTH DEVELOPMENT OF MINERAL ADMIXTURE INCORPORATED CALCIUM ALUMINATE CEMENTS**

Erkmen, Kadir Can  
MSc., Department of Civil Engineering  
Supervisor: Prof. Dr. Mustafa Tokyay

October 2018, 73 pages

Calcium aluminate cements (CACs) have very high early strength and high early heat evolution. On the other hand, at relatively high ambient temperatures and humidity the hydration products may convert into other products of lower binding value and porous structure which result in lower strength at later ages. In order to prevent such strength losses mineral admixtures such as ground granulated blast furnace slag and fly ash may be incorporated in CACs. In this respect, the main goal of this study was to obtain mechanically stable binder combinations by incorporating these mineral admixtures into CAC. The effects of these mineral admixtures on the hydration process and strength development of CAC blended cement pastes and mortars at different curing temperatures were investigated through calorimetry, XRD and strength tests. The hydration reactions found to be happening significantly faster at elevated temperatures. The presence of a sufficient amount of GGBFS in the blends at different curing temperatures proved to be helpful in terms of hindering strength losses, however there is not such a clear effect observed in fly ash containing binders.

Keywords: Calcium Aluminate Cement, Ground Granulated Blast Furnace Slag, Fly Ash, Hydration, Strength.



## ÖZ

### MİNERAL KATKILI KALSİYUM ALÜMİNAT ÇİMENTOSUNUN HİDRATASYON DAVRANIŞI VE DAYANIM GELİŞİMİ

Erkmen, Kadir Can  
Yüksek Lisans, İnşaat Mühendisliği  
Tez Yöneticisi: Prof. Dr. Mustafa Tokyay

Ekim 2018, 73 sayfa

Kalsiyum alüminat çimentoları (KAÇ) erken yüksek dayanıma sahiptirler ve yüksek hidrasyon ısıya açığa çıkarırlar. Öte yandan, yüksek sıcaklıklarda ve rutubetli ortamda hidrasyon ürünleri dönüşüme uğrayarak, gözenekli bir yapı oluşturarak, bağlayıcı özelliklerini önemli ölçüde kaybedebilmektedirler. Söz konusu dayanım kayıplarını önlemenin yollarından birisi KAÇ'ı granüle yüksek fırın cürufu ve uçucu kül gibi mineral katkılarla birlikte kullanmaktır. Bu bağlamda, bu çalışmanın ana amacı mineral katkıları ekleyerek mekanik olarak kararlı bağlayıcı kombinasyonları elde etmektir. Bu mineral katkıların farklı sıcaklıklarda kürlenmiş KAÇ içeren çimento hamurları ve harçlarının hidrasyonuna ve dayanım gelişimine etkileri kalorimetri, XRD ve dayanım deneyleriyle belirlenmiştir. Hidrasyon reaksiyonlarının yüksek sıcaklıklarda daha hızlı gerçekleştiği bulunmuştur. Çimento karışımında uygun miktarda öğütülmüş granüle yüksek fırın cürufu bulunmasının farklı kür sıcaklıklarında dayanım kayıplarını engelleme açısından faydalı olduğu ortaya çıkmıştır, ancak buna benzer açık bir etki uçucu kül içeren bağlayıcılarda gözlenmemiştir.

Anahtar Kelimeler: Kalsiyum Alüminat Çimentosu, Granüle Yüksek Fırın Cürufu, Uçucu Kül, Hidrasyon, Dayanım.

To My Parents, Ayşe and Muzaffer Erkmen



## ACKNOWLEDGEMENTS

I would like to express my great appreciation to my supervisor Prof. Dr. Mustafa Tokyay for his support, great guidance and supervision during the preparation of this thesis.

I am deeply grateful to my parents Ayşe and Muzaffer Erkmen and my sister İlke Erkmen for all their patience, encouragement and support throughout the study.

I am also grateful to my friends Baki Aykut Bilginer, Oğulcan Canbek and Mehmet Kemal Ardoğa for their their precious friendship and assistance in this study.

My sincere thanks are extended to ÇimSA Cement Production and Trade Company for supplying all the materials that I used in my thesis study.

I appreciate the assistance of the Materials of Construction Laboratory staff, especially Gülşah Bilici in the Department of Civil Engineering at METU.

The assistance of my work friends Arda Öcal, Halil İbrahim Andiç and Can Demir is also greatly appreciated.

I would like to thank my love Ayşe Bağcı for her endless love and all her patience, understanding and support throughout this research.

## TABLE OF CONTENTS

|   |      |
|---|------|
| ABSTRACT . . . . .  | v    |
| ÖZ . . . . .  | vi   |
| ACKNOWLEDGMENTS . . . . .                                   | viii |
| TABLE OF CONTENTS . . . . .                                 | x    |
| LIST OF TABLES . . . . .                                    | xiii |
| LIST OF FIGURES . . . . .                                   | xiv  |
| CHAPTERS  |      |
| 1 INTRODUCTION . . . . .                                    | 1    |
| 1.1 General . . . . .                                       | 1    |
| 1.2 Objective and Scope . . . . .                           | 2    |
| 2 THEORETICAL BACKGROUND AND LITERATURE REVIEW . . . . .    | 5    |
| 2.1 General . . . . .                                       | 5    |
| 2.2 Chemical and Mineralogical Composition of CAC . . . . . | 6    |
| 2.3 Physical Properties of CAC . . . . .                    | 8    |
| 2.4 Hydration of CAC . . . . .                              | 9    |
| 2.5 Conversion of Hydration Products of CAC . . . . .       | 10   |

|         |  |    |
|---------|--|----|
| 2.6     | Factors Influencing Conversion . . . . .               | 12 |
| 2.6.1   | Influence of Temperature . . . . .                     | 12 |
| 2.6.2   | Influence of Water-Cement Ratio . . . . .              | 15 |
| 2.7     | CAC Based Composite Systems . . . . .                  | 16 |
| 2.7.1   | CAC-GGBFS Binary System . . . . .                      | 16 |
| 2.7.2   | CAC-Fly Ash Binary System . . . . .                    | 21 |
| 3       | EXPERIMENTAL STUDY . . . . .                           | 25 |
| 3.1     | General . . . . .                                      | 25 |
| 3.2     | Materials . . . . .                                    | 25 |
| 3.2.1   | Mineralogical Composition . . . . .                    | 26 |
| 3.2.2   | Chemical Composition . . . . .                         | 27 |
| 3.2.3   | Density of Materials . . . . .                         | 28 |
| 3.2.4   | Fineness of Materials . . . . .                        | 28 |
| 3.3     | Mix Types and Mixing Protocols . . . . .               | 29 |
| 3.3.1   | Mix Types . . . . .                                    | 29 |
| 3.3.2   | Mixture Preparation . . . . .                          | 29 |
| 3.4     | Tests and Analyses Performed . . . . .                 | 30 |
| 3.4.1   | Analyses performed on cement pastes . . . . .          | 30 |
| 3.4.1.1 | Heat of Hydration . . . . .                            | 30 |
| 3.4.1.2 | X-Ray Diffraction Analyses . . . . .                   | 31 |
| 3.4.2   | Compressive strength tests of cement mortars . . . . . | 32 |

|       |  |    |
|-------|--|----|
| 4     | RESULTS AND DISCUSSION . . . . .                     | 33 |
| 4.1   | Effect of Temperature on Plain CAC . . . . .         | 33 |
| 4.1.1 | Effect on Heat of Hydration . . . . .                | 33 |
| 4.1.2 | Effect on Compressive Strength Development . . . . . | 34 |
| 4.1.3 | Effect on Microstructural Development . . . . .      | 37 |
| 4.2   | Effect of Temperature on CAC Blends . . . . .        | 41 |
| 4.2.1 | Effect on Heat of Hydration . . . . .                | 41 |
| 4.2.2 | Effect on Compressive Strength Development . . . . . | 48 |
| 4.2.3 | Effect on Microstructural Development . . . . .      | 59 |
| 5     | CONCLUSIONS AND RECOMMENDATIONS . . . . .            | 67 |
|       | REFERENCES . . . . .                                 | 71 |

## LIST OF TABLES

### TABLES

|           |  |    |
|-----------|--|----|
| Table 2.1 | Chemical compositions of different calcium aluminate cements [1]                 | 7  |
| Table 2.2 | Physical and mechanical properties of ISIDAÇ40 [2, 3]                            | 9  |
| Table 2.3 | Crystal Systems and Densities of Calcium Aluminate Hydrates [4]                  | 10 |
| Table 2.4 | Properties of reference and TFA (Treated Fly Ash) mortars [5]                    | 22 |
| Table 3.1 | Chemical Compositions of Materials   | 28 |
| Table 3.2 | Densities of materials   | 28 |
| Table 3.3 | Fineness of materials  | 29 |
| Table 3.4 | Mixture designations   | 29 |
| Table 4.1 | Compressive Strength Values of Plain CAC Cured at 20, 40, 60°C (MPa)             | 35 |
| Table 4.2 | Compressive Strength Values of Plain CAC and CAC Blend Mixes Cured at 20°C (MPa) | 48 |
| Table 4.3 | Compressive Strength Values of Plain CAC and CAC Blend Mixes Cured at 40°C (MPa) | 49 |
| Table 4.4 | Compressive Strength Values of Plain CAC and CAC Blend Mixes Cured at 60°C (MPa) | 49 |

## LIST OF FIGURES

### FIGURES

|   |    |
|---|----|
| Figure 2.1 The progress of conversion based on temperature and its relation with strength[6] . . . . .  | 13 |
| Figure 2.2 The effect of temperature on the rate of conversion and strength development[7] . . . . .  | 13 |
| Figure 2.3 XRD patterns of CACs at 3 days of curing at temperatures a) 5°C b) 20°C c) 40°C [8] . . . . .  | 14 |
| Figure 2.4 The effect of water-cement ratio on CAC concrete at high and low water-cement ratios cured at 20°C [7] . . . . .                             | 15 |
| Figure 2.5 The influence of the replacement level of GGBFS and curing temperature on the strength of CAC-GGBFS mixes [9] . . . . .                      | 17 |
| Figure 2.6 XRD patterns of mixes prepared with 40% GGBFS replacement at different curing temperatures [9] . . . . .                                     | 17 |
| Figure 2.7 XRD patterns of air cooled and water cooled slag incorporated calcium aluminate cements cured at 40°C [10] . . . . .                         | 18 |
| Figure 2.8 Compressive strength development of CAC and slag incorporated CAC pastes up to the curing age of 28 days [11] . . . . .                      | 19 |
| Figure 2.9 Compressive strength development of 1:1 ratio of CAC to GGBFS mixes cured at 20°C [12] . . . . .   | 20 |
| Figure 2.10 Compressive strength development of 50% CAC - 50% GGBFS blends up to ten years [13] . . . . .   | 20 |
| Figure 2.11 The rate of heat evolution curves of pastes with the replacement of different additives a) 5% of additive b) 25% of additive [14] . . . . . | 21 |
| Figure 2.12 Strength development of mortars prepared with the partial 20% replacement of fly ash [15] . . . . .   | 23 |

|  |    |
|--|----|
| Figure 2.13 Strength development of mortars prepared with the partial 40% replacement of fly ash [15] . . . . .  | 23 |
| Figure 2.14 XRD analysis for mortars containing 20 mass% fly ash at the curing age of 300 days [15] . . . . .  | 24 |
| Figure 3.1 XRD Pattern of CAC . . . . .  | 26 |
| Figure 3.2 XRD Pattern of GGBFS . . . . .  | 26 |
| Figure 3.3 XRD Pattern of Fly Ash . . . . .  | 27 |
| Figure 4.1 Rate of Heat Evolution of Plain CAC at Three Different Curing Temperatures . . . . .  | 34 |
| Figure 4.2 Compressive Strength Development of Plain CAC at Three Different Curing Temperatures . . . . .  | 35 |
| Figure 4.3 1-day strength and change in strength at 180 days at different curing temperatures . . . . .  | 37 |
| Figure 4.4 XRD Patterns of plain CAC pastes cured at 20°C . . . . .  | 38 |
| Figure 4.5 XRD Patterns of plain CAC pastes cured at 40°C . . . . .  | 38 |
| Figure 4.6 XRD Patterns of plain CAC pastes cured at 60°C . . . . .  | 39 |
| Figure 4.7 XRD patterns of CAC samples hydrated for 1 day at 20°C, 40°C, and 60°C . . . . .  | 41 |
| Figure 4.8 Rate of Heat Evolution of CAC-GGBFS mixes cured at 20°C . . . . .   | 43 |
| Figure 4.9 Rate of Heat Evolution of CAC-FA mixes cured at 20°C . . . . .  | 43 |
| Figure 4.10 Comparative rates of heat flow in acceleration stage for (a) slag-incorporated and (b) fly ash-incorporated pastes cured at 20°C . . . . . | 44 |
| Figure 4.11 Rate of Heat Evolution of CAC-GGBFS and CAC-FA mixes cured at 40°C . . . . .   | 45 |
| Figure 4.12 Rate of Heat Evolution of CAC-GGBFS and CAC-FA mixes cured at 40°C during the acceleration stage . . . . .                                 | 46 |
| Figure 4.13 Rate of Heat Evolution of CAC-GGBFS and CAC-FA mixes cured at 60°C . . . . .   | 47 |
| Figure 4.14 Age-strength relations for slag-incorporated CAC mortars in comparison with pure CAC mortars cured at 20°C . . . . .                       | 50 |

|   |    |
|---|----|
| Figure 4.15 Age-strength relations for fly ash-incorporated CAC mortars in comparison with pure CAC mortars cured at 20°C . . . . . | 50 |
| Figure 4.16 Age-strength relations for slag-incorporated CAC mortars in comparison with pure CAC mortars cured at 40°C . . . . .    | 51 |
| Figure 4.17 Age-strength relations for fly ash-incorporated CAC mortars in comparison with pure CAC mortars cured at 40°C . . . . . | 51 |
| Figure 4.18 Age-strength relations for slag-incorporated CAC mortars in comparison with pure CAC mortars cured at 60°C . . . . .    | 52 |
| Figure 4.19 Age-strength relations for fly ash-incorporated CAC mortars in comparison with pure CAC mortars cured at 60°C . . . . . | 52 |
| Figure 4.20 Effect of slag(S) or fly ash(F) incorporation on 1 day strength at 20°C   | 54 |
| Figure 4.21 XRD traces of CAC and S- and F-incorporated pastes hydrated for 1 day at 20°C . . . . .                                 | 54 |
| Figure 4.22 XRD traces of CAC and S- and F-incorporated pastes hydrated for 180 days at 20°C . . . . .                              | 55 |
| Figure 4.23 180 days to 1 day strength ratios of mortars cured at 20°C . . . . .  | 56 |
| Figure 4.24 Effect of slag(S) or fly ash(F) incorporation on 1-day strength at 40°C . . . . .                                       | 57 |
| Figure 4.25 XRD traces of GGBFS and fly ash incorporated pastes hydrated for 1 day at 40°C . . . . .                                | 58 |
| Figure 4.26 180 days to 1 day strength ratios of mortars cured at 40°C . . . . .  | 58 |
| Figure 4.27 180 days to 1 day strength ratios of mortars cured at 60°C . . . . .  | 59 |
| Figure 4.28 XRD Patterns of S20 Pastes cured at 20°C . . . . .  | 60 |
| Figure 4.29 XRD Patterns of S60 Pastes cured at 20°C . . . . .  | 60 |
| Figure 4.30 XRD Patterns of F20 Pastes cured at 20°C . . . . .  | 61 |
| Figure 4.31 XRD Patterns of S20 Pastes cured at 40°C . . . . .  | 62 |
| Figure 4.32 XRD Patterns of S60 Pastes cured at 40°C . . . . .  | 62 |
| Figure 4.33 XRD Patterns of F20 Pastes cured at 40°C . . . . .  | 63 |
| Figure 4.34 XRD Patterns of S20 Pastes cured at 60°C . . . . .  | 64 |
| Figure 4.35 XRD Patterns of S60 Pastes cured at 60°C . . . . .  | 64 |



Figure 4.36 XRD Patterns of F20 Pastes cured at 60°C . . . . . 65



# CHAPTER 1

## INTRODUCTION

### 1.1 General

Different cement types have different characteristics. Of the different cement types, portland cement is the most widely known one as well as being the mostly used. On the other hand, calcium aluminate cement (CAC) is among the various types of cements and differs mostly from the portland cement due to its chemical composition. CAC contain much more alumina and in that respect less silica as opposed to portland cement. For this reason, CACs are also labelled as high alumina cements in a number of sources. Likewise, the term "Ciment Fondu" can be thought as the french word for CAC. The patent of CAC was taken by Jules Bied from the J. and A. Pavin de Lafarge company [1, 6]. It originated at the beginning of 1900s after the First World War [1, 6].

As CAC contain more alumina, varying over a range of 40% to 80%, compared to portland cement, using CAC can sometimes be quite advantageous [16, 17]. To illustrate, using CACs can provide a bunch of benefits such as rapid strength gain, high abrasion resistance and rapid setting behavior. When these benefits are taken into account, special applications that require the existence of above-mentioned properties may favor the use of high alumina cements. However, using CAC can also be problematic as its hydration products are transformed into other products which creates a significant amount of strength loss[9]. That is why use of CAC was limited due to the strength losses observed and reported in structural concrete. Failures of structures limited the use of CAC at those times.

As explained in the previous paragraph, hydration products that occur during the calcium aluminate cement hydration process have the potential to turn out to be other products that may well pose a threat in terms of strength development. To prevent the plausible detrimental effects of this conversion, CAC might be blended with mineral admixtures [9]. There are many mineral admixtures currently utilized in concrete production ranging from natural materials to pozzolans which are indeed by-products obtained from industrial activities. Using mineral admixtures provides a bunch of advantages such as reducing the heat of hydration, boosting the sulfate resistance of concrete, enhancing the ultimate strength and so forth. Under certain circumstances, the reaction between pozzolanic materials, calcium hydroxide and water brings about the formation of new CSH gels which later leads to an enhanced strength. Some of the previous studies have demonstrated that microsilica, ground granulated blast furnace slag and fly ash are quite favored for the purpose of blending CAC with different admixture types [18].

## **1.2 Objective and Scope**

The objective of this study is to determine how mineral admixture incorporation affects the hydration and strength behavior of calcium aluminate cement. For this purpose, two mineral admixtures -GGBFS and fly ash- were used to partially replace CAC at different ratios. As a result of this, binary systems involving CAC and either of the mineral admixture were studied.

During the phases of this research, mineral admixture incorporated cements were subjected to three different curing temperatures. Continuous moist curing at 20°C, 40°C and 60°C were applied for each of the mixtures. To monitor how strength development occurs, compressive strength tests were applied at certain ages starting from 1 day up to 180 days. In this respect, XRD analyses and isothermal conduction calorimetry method were used with the aim of explaining the early hydration behavior of mixtures as well as the changes occurring on the microstructural level in parallel with strength development. A total of 7 mixtures were tried to be compared with one another while consideration paid to different curing modes.

This thesis is composed of six chapters,

Chapter 1 provides general information about calcium aluminate cement and its chemical and mechanical behavior. Moreover, objective of this study and its scope are also presented.

Chapter 2 presents the theoretical background and literature review to provide a background and literature review to provide a background information about CAC, mineral admixtures and their use together.

Chapter 3 mainly explains the experimental study encompassing the materials used and the experiment carried out.

Chapter 4 is devoted to the results and discussion, the findings of this study are presented and discussed in this chapter.

Chapter 5 presents the conclusion by summarizing the chief findings and critical points found in this study.

Chapter 6 is devoted to the recommendations for future studies.



## CHAPTER 2

# THEORETICAL BACKGROUND AND LITERATURE REVIEW

### 2.1 General

Compared to portland cements, CACs have some significant advantages and also unique features which make CACs a key aspect of certain applications. Among all of its features, high early rate of strength gain might be the most valuable one. Despite CACs normal setting times, their 24h strength value is equivalent to the strength value of portland cement in 28 days. Boosted abrasion resistance especially at low temperatures is also a strong side of CACs [1, 6]. Similarly, CACs show good resistance to various durability problems particularly the ones such as sulphate attack and alkali-silica reaction [4, 6].

Nowadays CACs are commonly utilized to make refractory concretes. The role of CACs in refractory concretes is being a binder and the type of binder has the potential to influence significant characteristics of the refractory concretes. Consideration paid to the afore-mentioned statements where properties of CACs are outlined, the applications regarding its use can be listed as follows [1]:

- Since the speed of hydration reaction is quite fast in CACs, it can be used in constructions where weather conditions are harsh during winter times.
- As CACs are considerably resistant to chemical abrasions, it can be used in inner coating of sewer systems.
- If there are structures that need to go into service in a short span of time, CACs

become more than just a choice due to their high early strength gain rate and rapid hardening characteristics.

- When combined with suitable refractory aggregates, making refractory castables is quite possible with the aid of CACs.
- If biological and acidic attacks are expected to occur in some certain applications like tunnels, industrial floors and pipes CACs can also be preferred.
- Calcium aluminate cements can be mixed with portland cements in order to be used for applications such as grouting where rapid setting mixtures are required.

## 2.2 Chemical and Mineralogical Composition of CAC

CAC is a cement type which is preferred in special applications and having some unique features. During its manufacture, limestone and bauxite make up CAC under complete fusion. Compared to portland cement, it contains much more alumina but less silica at the same time. When portland cement reacts with water and as hydration progresses, clinker phases  $C_3S$ ,  $C_2S$ ,  $C_3A$  and  $C_4AF$  generate calcium silicate hydrate gels, calcium hydroxide and calcium-alumino-sulfo hydrates. In this respect, as distinct from the hydration products of portland cement, calcium oxide and alumina present in CACs create calcium aluminate hydrates and  $CA$ , which is the most significant one among them, is responsible for strength development. Depending upon the alumina content, CACs are named differently and CACs having different chemical compositions are summarized in Table 2.1 [1]. CACs consisting 40% Alumina are the most commonly used ones and the others having higher alumina are often preferred for special applications like abrasion resistance or refractoriness.

The expected crystalline phases in CACs are  $CA$ ,  $C_{12}A_7$ ,  $\beta$ - $C_2S$ ,  $C_2AS$ ,  $C_4AF$ . In addition to these, pleochroite and perovskite( $CaTiO_3$ ) are the minor phases that can possibly be seen [1].  $CA$  (monocalcium aluminate) is the chief and most significant phase that is present in all high alumina cements and provides the cementitious property to CAC. It is the phase that constitutes approximately half of the cement clinker. Monocalcium aluminate hydrate development is more likely to occur at low temperatures and crystallizes like hexagonal prisms [19].



Table 2.1: Chemical compositions of different calcium aluminate cements [1]

| Type of cement | $Al_2O_3$ | $CaO$ | $FeO$<br>+<br>$Fe_2O_3$ | $FeO$ | $SiO_2$ | $TiO_2$ | $MgO$ | $K_2O$<br>+<br>$Na_2O$ | $SO_3$ |
|----------------|-----------|-------|-------------------------|-------|---------|---------|-------|------------------------|--------|
| Ciment Fondu   | 38-40     | 37-39 | 15-18                   | 3-6   | 3-5     | 2-4     | <1.5  | <0.4                   | <0.2   |
| 40% Alumina    | 40-45     | 42-48 | <10                     | <5    | 5-8     | 2       | <1.5  | <0.4                   | <0.2   |
| 50% Alumina    | 49-55     | 34-39 | <3.5                    | <1.5  | 4-6     | 2       | 1     | <0.4                   | <0.3   |
| 70% Alumina    | 69-72     | 27-29 | <0.3                    | <0.2  | <0.8    | <0.1    | <0.3  | <0.5                   | <0.3   |
| 80% Alumina    | 79-82     | 17-20 | <0.25                   | <0.2  | <0.4    | <0.1    | <0.2  | <0.7                   | <0.2   |

$C_{12}A_7$  (dodecacalciumheptaaluminate) is an extremely reactive mineral and as soon as subjected to  $H_2O$  it changes rapidly to hydrated calcium aluminates [20]. With  $C_{12}A_7$  present in high amounts in cement, it can cause a great deal of expansion as it is highly reactive. For this reason, the presence of  $C_{12}A_7$  is not preferable however, a small amount of it usually exists [21]. Dicalcium silicate development in Portland cement is in metastable  $\beta$  pattern then becomes stable with the aid of impurities [22]. Hydration characteristics of  $\beta$ - $C_2S$  resemble  $C_3S$  with a difference as  $\beta$ - $C_2S$  hydrate in a slower fashion. This feature is attributed to the different crystalline structure of  $\beta$ - $C_2S$  [22].  $C_2AS$  (gehlenite) is classified under the melilite group and it is known to be only weakly reactive [4]. Therefore,  $C_2AS$  does not contribute much to the hydration process in the beginning however, its contribution starts at later stages. In this respect,  $C_2AS$  shows a somewhat similar behavior to  $C_2S$ . Among all phases,  $C_4AF$  (ferrite) phase changes from 20% to 40% in high alumina cements depending upon the amount of  $Fe_2O_3$  present in the raw mix [17]. Thus, after  $CA$  (monocalcium aluminate), ferrite phase constitute a significant portion of CAC clinker phases. In CACs, the role of ferrite phase in early hydration is almost none at 20°C however, a significant amount of it was observed to react by 2 months at temperatures 30 – 38°C [1]. This phase cannot be encountered in white high alumina cements that are free of iron. Pleochroite is also a phase that may possibly be seen in some calcium aluminate cements but found to be unreactive [1]. In calcium aluminate liquid if highly soluble

titanium is in question than the crystallisation of a perovskite phase is likely to be formed [4].

### 2.3 Physical Properties of CAC

The color of CAC mostly depends on two factors which can be named as the iron content of the cement as well as the alumina content of it. High alumina cements which have alumina contents over 70% are mostly white whereas the others that have comparatively less alumina content have a dark grey colour whose tone is governed by the iron content.

The setting times of portland cement and calcium aluminate cements show similar characteristics and the setting time of calcium aluminate cement changes between 3 and 5 hours [7]. However as lime to alumina ratio decreases, setting time values start to be much longer. One of the phases present in CACs is  $C_{12}A_7$  which is a lime-rich phase leads to the presence of shorter setting times and for this reason,  $C_{12}A_7$  amount is controlled within the limits during the production stage [7]. Apart from these statements, setting times of CACs are also highly dependent upon the temperature. Most CACs reach maximum setting time values at temperatures 25 – 30°C and at temperatures between 0°C to 20°C as well as above 30°C, swift shortening of the setting time values are observed [1].

The rate of hydration and hardening for CACs are quite high and in this respect, high compressive strength values in CAC concretes can be easily obtained in early stages like at 6 to 24 hours. A natural outcome of this high reactivity is obtaining high heat of hydration values over a short period of time. Although high temperatures are seen during the hydration process, CAC concretes do not show solid evidence of serious thermal cracking and this may be attributed to the relaxation of thermally induced strains as a result of facilitated creep [7]. This facilitated creep may stem from the conversion reactions of initially formed calcium aluminate hydrates and low stress-strain rate of the nature of CAC concretes [7].

Specific gravity values of CAC depend on the iron content and directly proportional to that as well. As an average or standard value 3200-3250 kg/m<sup>3</sup> can be stated which

is a little greater than Portland cement specific gravity values. Blaine fineness values have a range of 250-400  $m^2/kg$  however for CACs with higher  $Al_2O_3$  contents, the fineness value might go up to 1000  $m^2/kg$  [4].

Soundness tests for CACs do not seem to be relevant as they involve no free lime and only very small amount of magnesium oxide [4]. Physical and mechanical properties of calcium aluminate cements produced in Turkey are outlined in TS EN 14647. In this respect, Table 2.2 shows physical and mechanical properties of ISIDAÇ40 which is produced by ÇİMSA, as the sole manufacturer of CAC in Turkey [2, 23, 3].

Table 2.2: Physical and mechanical properties of ISIDAÇ40 [2, 3]

| Physical and Mechanical Properties | Unit     | Value |
|------------------------------------|----------|-------|
| Specific Weight                    | $g/cm^3$ | 3.25  |
| Blaine Fineness                    | $cm^2/g$ | 3000  |
| Flow Test (w/c:0.45) (ASTM C-109)  | %        | 55    |
| Initial Set                        | min.     | 280   |
| Final Set                          | min.     | 295   |
| Volume Stability (Le Chatelier)    | mm       | 1.0   |
| Residue on 0.045 mm Sieve          | %        | 23.0  |
| Residue on 0.090 mm Sieve          | %        | 6.5   |
| 6 hour compressive strength        | MPa      | 47.0  |
| 24 hour compressive strength       | MPa      | 70.0  |

## 2.4 Hydration of CAC

The chemical exothermic reaction between cement and water is known as hydration. A similar mechanism to portland cement hydration for calcium aluminate cements is valid where the hydrate phases take the place of anhydrous cement and water creating a greater amount of solid volume. Despite this similarity, hydration products of the above-mentioned cements are not alike[7]. Different hydration products may occur chiefly depending on temperature and the hydration of main constituents of CAC which are namely,  $CA$  and  $C_{12}A_7$ .

Hydration in calcium aluminate cements starts with dissolution and continues with precipitation process[7, 4]. Following the addition of water,  $CA$  and  $C_{12}A_7$  dissolve

as the anhydrous phases to produce  $Ca^{2+}$  and  $Al(OH)^{-4}$  ions in the solution[7, 4]. These ions come together to create calcium aluminate hydrates or aluminate hydrates which are namely  $CAH_{10}$ ,  $C_2AH_8$ ,  $C_3AH_6$  and  $AH_3$ . Crystal systems and density values of the above-mentioned calcium aluminate hydrates are shown in Table 2.3 [4].

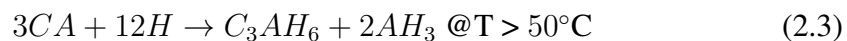
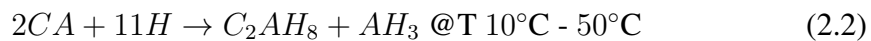
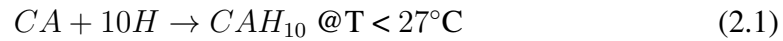
Table 2.3: Crystal Systems and Densities of Calcium Aluminate Hydrates [4]

| Calcium Aluminate Hydrates | $CAH_{10}$ | $C_2AH_8$ | $C_3AH_6$ | $AH_3$     |
|----------------------------|------------|-----------|-----------|------------|
| Crystal System             | Hexagonal  | Hexagonal | Cubic     | Monoclinic |
| Density ( $kg/m^3$ )       | 1720       | 1950      | 2520      | 2400       |

To explain the hydration mechanism in a more precise way, the following can be stated. At the initial stage, upon contact with water, precipitation of hydrates is not applicable even if the solution concentration reaches the critical supersaturation point of  $C_2AH_8$  or  $AH_3$  as it drops from that level later on[4]. Thus, no notable precipitation occurs for any of these two phases. During the induction period, nuclei grows and reaches a critical size and following that precipitation happens to a huge extent where the solution concentration fall to the hydrate solubility curves[4].

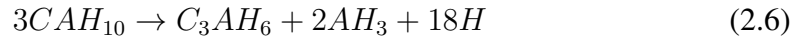
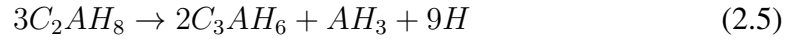
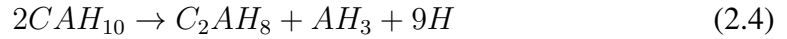
## 2.5 Conversion of Hydration Products of CAC

Two major phases of CAC are  $CA$  and  $C_{12}A_7$  whose hydration reactions are somewhat analogous[4]. As explained earlier, the formation of hydration products of CAC is largely affected by the temperature. In this respect, the following reactions 2.1, 2.2, 2.3 belongs to the hydration of  $CA$  and similarly  $C_{12}A_7$ .



As a result of reactions, new phases which have a tendency to possess the lowest possible energy occur[7]. They are called stable phases however, the formation of stable phases is not always likely because of the nucleation process thus, temporary phases occur that can be named as metastable phases. Due to the energy differences, a force still exists that can cause stable phase formation later on[7]. As it can be seen from Figure 2.1,  $CAH_{10}$  formation continues up to temperatures about  $27^{\circ}\text{C}$  and especially at temperatures below  $10^{\circ}\text{C}$ ,  $CAH_{10}$  becomes the dominating hydration product. Between the curing temperatures of  $10^{\circ}\text{C}$  and  $27^{\circ}\text{C}$ , both  $CAH_{10}$  and  $C_2AH_8$  form however,  $CAH_{10}$  formation is more favored. At temperatures above  $28^{\circ}\text{C}$ ,  $CAH_{10}$  does not form and instead  $C_2AH_8$  or  $C_3AH_6$  formation can be seen. On the other hand, at elevated temperatures above  $50^{\circ}\text{C}$ , a stable phase  $C_3AH_6$  occurs at early hydration stages and this product may well be the only phase at these temperatures[4, 6, 17].

As explained in the previous paragraph, metastable phases tend to convert into the stable ones and that takes place over time. As a result, metastable products which are  $CAH_{10}$  and  $C_2AH_8$  convert into stable  $C_3AH_6$  as shown in 2.4, 2.5 and 2.6.



The rate of conversion reactions are affected by a number of factors such as temperature, relative humidity and water-cement ratio. The major influence of conversion is the change it creates on the level of porosity. If the amounts of water and space are at adequate levels, anhydrous phases produce metastable hydrates as a consequence of hydration reaction. Following that as metastable hydrates own low solid density, pores are filled with them. However, when conversion takes place, the porosity increases since stable hydrates are comparatively more dense and cannot fill the pores

as much as metastable ones. With regard to the increase in porosity, a decreasing trend in strength is observed[7].

Another impact of conversion on CACs is the volume changes that happen during the hydration process. The amount of volume change that occurs can be found by calculating the densities of the hydrated phases[1, 4]. The volume changes are dependent upon the conversion of either  $CAH_{10}$  phase or  $C_2AH_8$ . During the conversion reactions if the first product forming is  $CAH_{10}$ , the total volume of the solids reduces by approximately 50% of the initial value whereas the change becomes 75% if the mixture consists of  $C_2AH_8$  and  $AH_3$ [1]. On the other hand, subsequent to conversion, a decent amount of water is released meaning that the remaining water can provide a way for further hydration. With further hydration, the residual anhydrous cement goes into the reaction bringing about an increase in total solid volume. Surely, the above-mentioned points are related to water-cement ratio as well if high water-cement ratio exists, the amount of cement that can hydrate at the beginning are boosted so that the impact of conversion is appreciably greater in terms of porosity and strength related to that.

## **2.6 Factors Influencing Conversion**

Two important factors influencing conversion are temperature and water-cement ratio. Especially, both curing and ambient temperature are quite critical for the rate of conversion reactions in CAC as they are governing parameters. Besides that, water-cement ratio is also significant as the water present directly affects the hydration reaction and conversion subsequently. The effects of these two elements are explained in the following sections.

### **2.6.1 Influence of Temperature**

It is known that the formation of different types of calcium aluminate hydrates are heavily dependent on curing and ambient temperature. At high temperatures, the stable  $C_3AH_6$  phase forms during the initial stages of hydration thus, a conversion may not even be the case. At relatively low temperatures, the rate of conversion is directly

proportional to the temperature value. The more temperature becomes the more conversion rate can be observed. The progress of conversion based on temperature and its relation with strength is illustrated in Figure 2.1 [6].

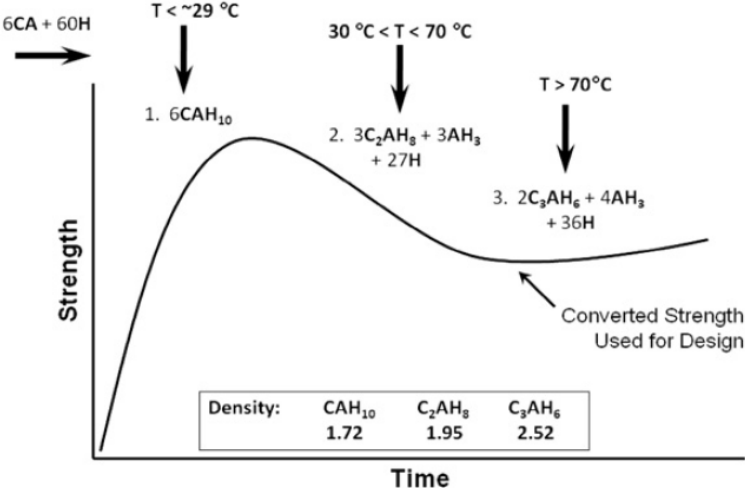


Figure 2.1: The progress of conversion based on temperature and its relation with strength[6]

On the other hand, the effect of temperature on the rate of conversion and strength development is illustrated in Figure 2.2 [7].

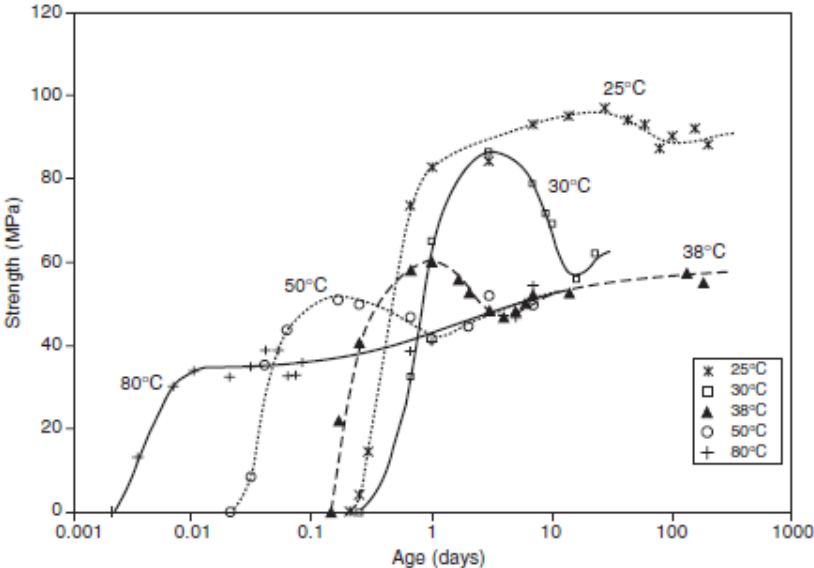


Figure 2.2: The effect of temperature on the rate of conversion and strength development[7]

As it can be seen from Figure 2.2, at temperatures above 50°C, stable hydrates form very rapidly as increasing temperatures speed up the rate of conversion. Likewise, the minimum strength value occurs around 24 hours at 50°C and conversion happens even within hours at temperatures above 50°C. To compare different temperature values and minimum strength, it can be said that the minimum strength is attained at 5 days at a curing temperature of 38°C.

Antonovic et al. studied the relation between the formation of calcium aluminate hydrates at three different curing temperatures 5°C, 20°C and 40°C. In this respect, it was observed that at 5°C  $CAH_{10}$  formed solely whereas  $CAH_{10}$  and  $C_2AH_8$  formed together at 20°C and  $C_3AH_6$  and  $AH_3$  were the main hydration products at 40°C. In addition to that, unhydrated  $CA$  and  $CA_2$  were observed heavily at 5°C and partially at 20°C however, none of them were observed at 40°C. Related XRD patterns of CACs at 3 days of curing at temperatures 5°C, 20°C and 40°C are illustrated in Figure 2.3 [8].

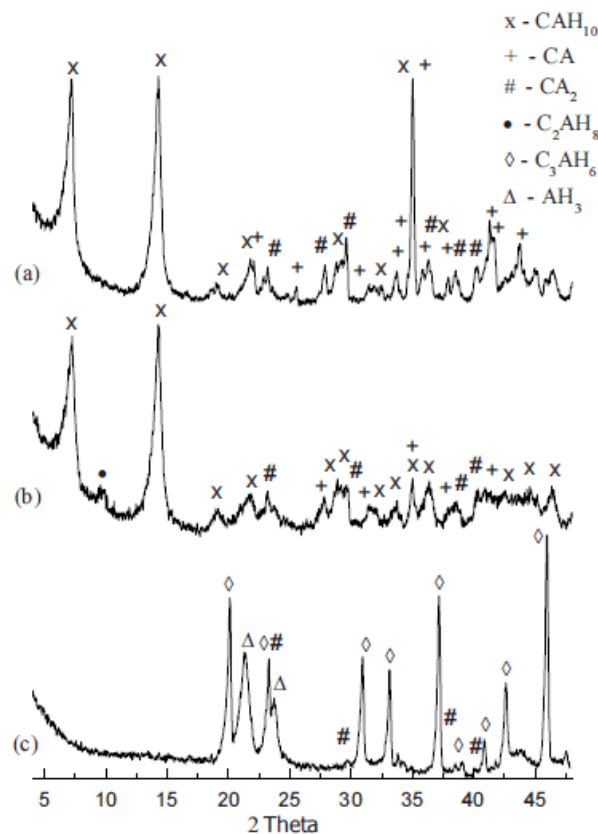


Figure 2.3: XRD patterns of CACs at 3 days of curing at temperatures a) 5°C b) 20°C c) 40°C [8]



## 2.6.2 Influence of Water-Cement Ratio

The effect of water-cement ratio on the behavior of CACs is critical as it directly affects the formation of hydration products as well as the conversion possibly. Even though the conversion is highly temperature dependent, water-cement ratio plays a significant role in this process as well. In this respect, after the researches carried out together with laboratory testing, recommended water-cement ratios were proposed. The most common value stated by manufacturers is 0.4 therefore, water-cement ratios that are greater than 0.4 are not recommended to be used. Using higher water-cement ratios than the recommended value may produce misleading results because high unconverted strength values can be obtained this way. However, these values are not truly representative since they do not reflect the actual ultimate strength that is attained. The reason behind this is that used high water-cement ratios will ultimately cause a reduction in strength because of conversion. The effect of water-cement ratio on CAC concrete at high and low water-cement ratios are shown in Figure 2.4 [7].

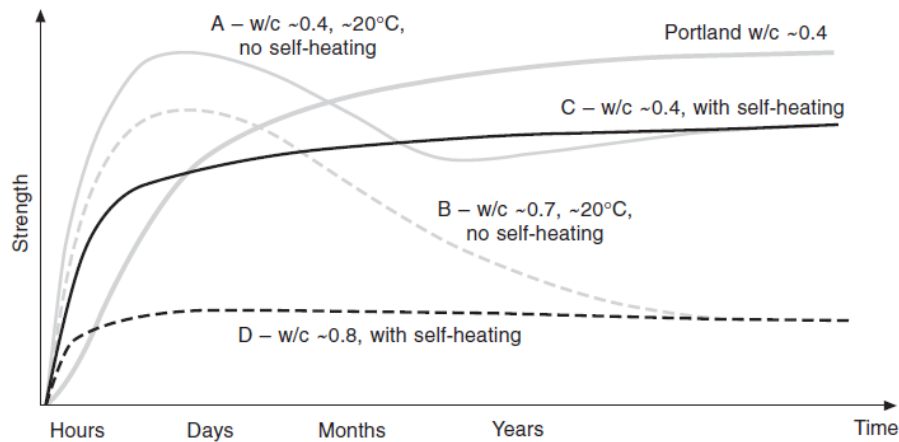


Figure 2.4: The effect of water-cement ratio on CAC concrete at high and low water-cement ratios cured at 20°C [7]

As it can be seen from Figure 2.4, when A and B are compared, which are under the same conditions except for water-cement ratios, B possessing a higher water-cement ratio experiences dramatic changes in strength even after a long time of curing. As opposed to that, despite A undergoes a slight strength loss, its strength becomes stable after a certain point.

## 2.7 CAC Based Composite Systems

Calcium aluminate cements are useful in a lot of application areas however, reported reductions in strength in the last few decades damaged their reputation. This reduction in strength is known to stem from the conversion of metastable hydration products of calcium aluminate cements. To prevent this, using cement replacement materials along with these cements was thought to be potentially useful. Later on, it was found that reactive silica found in pozzolanic materials prevents the conversion process as a result of the formation of stable product called *straetlingite* [7, 4, 1, 9, 15, 24, 13, 25, 10] In that respect, calcium aluminate cement based systems including fly ash, ground granulated blast furnace slag, silica fume and so on have been studied thoroughly.

### 2.7.1 CAC-GGBFS Binary System

A number of researches have been carried out on blended high alumina cement systems and most of them concentrated on CAC-GGBFS system in particular. The silica present in GGBFS alters the formation of hydration products as it provokes the formation of *straetlingite*. *Straetlingite* forms instead of metastable compounds  $CAH_{10}$  and  $C_2AH_8$  and creates a stable system as a result [9, 13, 12, 10, 11]. Therefore, if a proper amount of GGBFS replacement of CAC is done, the binary system can show a steady strength increase as opposed to pure CAC systems where the decrease of strength is characteristic.

Kirca et al. reported that GGBFS blended CAC systems prevent the conversion process especially where GGBFS replacement ratio is over 40% [9, 26]. When GGBFS became the main component in the blended system, *straetlingite* formation was boosted. In parallel with that, any decline of strength during the test ages was not also seen. In light of the above information, the influence of the replacement level of GGBFS and curing temperature on the strength of CAC-GGBFS mixes is illustrated in Figure 2.5 [9]. Additionally, XRD patterns of mixes prepared with 40% GGBFS replacement at different curing temperatures are illustrated in Figure 2.6 at 28 days and 210 days of curing time [9].

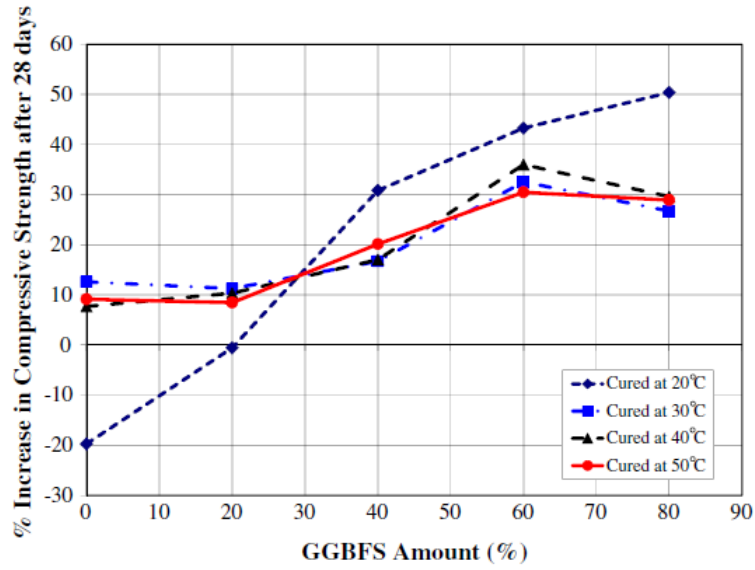


Figure 2.5: The influence of the replacement level of GGBFS and curing temperature on the strength of CAC-GGBFS mixes [9]

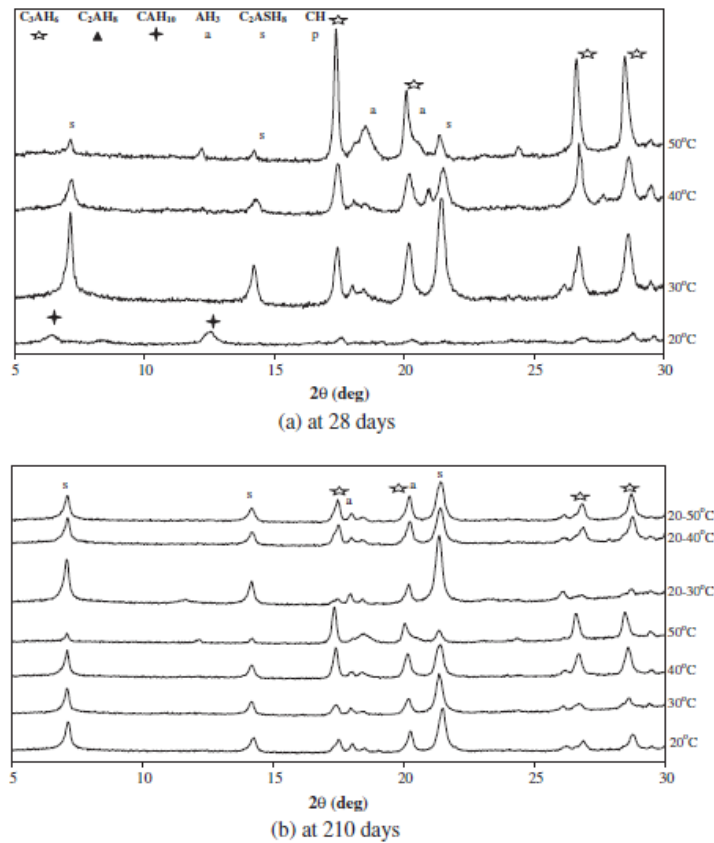


Figure 2.6: XRD patterns of mixes prepared with 40% GGBFS replacement at different curing temperatures [9]

As seen in Figure 2.6, the type of hydration products formed at 28 days highly depend on temperature. The formation of  $C_3AH_6$  seems to be enhanced at elevated temperatures thus, the presence of straeltingite was not quite strong. However, at 210 days the conversion seems to be completed as either stable  $C_3AH_6$  or straeltingite formed at all temperatures. The amount of straeltingite present depends on the amount of GGBFS used as well as the curing temperature [9].

In the study of Heikal et al., XRD patterns of air cooled and water cooled slag incorporated calcium aluminate cements cured at 40°C were investigated which are shown in Figure 2.7. Similar results to Kırca et al. were also reported in this study where stable hydrates  $C_3AH_6$  and  $C_2ASH_8$  (straeltingite) coexisted. These results are consistent with their reported compressive strength results. Therefore, it can be concluded that compressive strength values rise if air cooled or water cooled slag is incorporated into pure CAC [10].

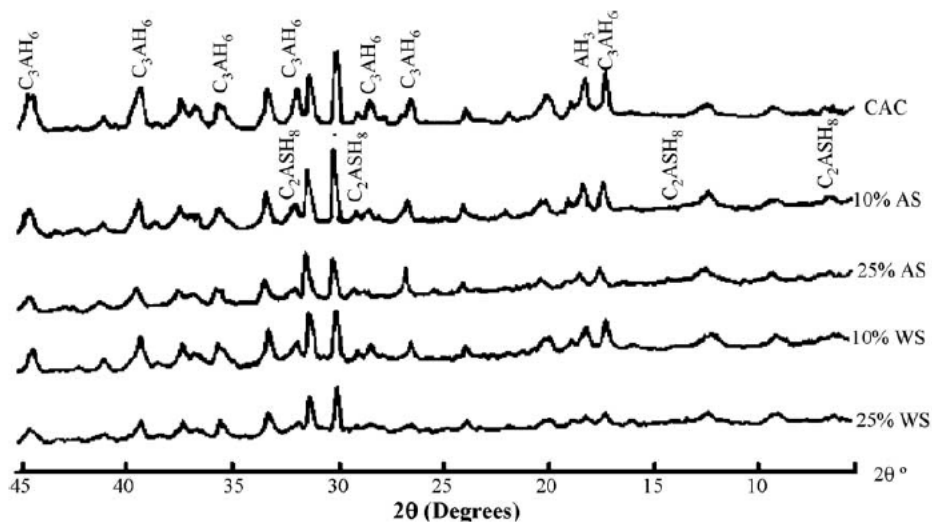


Figure 2.7: XRD patterns of air cooled and water cooled slag incorporated calcium aluminate cements cured at 40°C [10]

According to another study carried out by Heikal et al., compressive strength developments of pure CAC pastes and the ones containing air cooled or water cooled slag are compared with one another. Formerly derived conclusion touched on in the previous paragraph which is the presence of slag results in higher strength values was proven in this research as well [10, 11]. Compressive strength development of pastes

up to the curing age of 28 days is illustrated in Figure 2.8 [11].

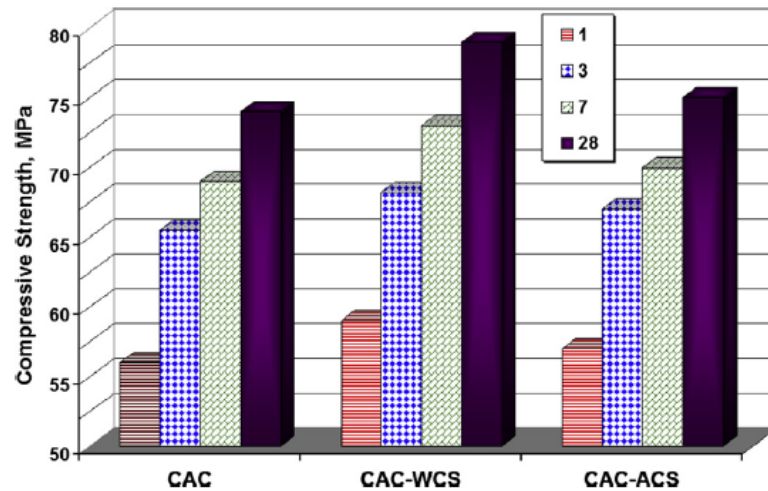


Figure 2.8: Compressive strength development of CAC and slag incorporated CAC pastes up to the curing age of 28 days [11]

Quillin et al. investigated how water-cement ratio, curing temperature and conditions affect the strength development of CAC-GGBFS blends specifically 1:1 ratio of CAC to GGBFS. Pastes having smaller water-cement ratios demonstrated more swift strength development and water cured samples also possessed higher strength values especially at later ages compared with the air cured ones. On the other hand, X-Ray diffraction patterns of all samples included strong peaks of  $C_2ASH_8$  (straelingite) except for the mix prepared with a water-cement ratio of 0.35 and air stored [12]. Figure 2.9 shows the compressive strength development of 1:1 ratio of CAC to GG-BFS mixes cured at 20°C [12].

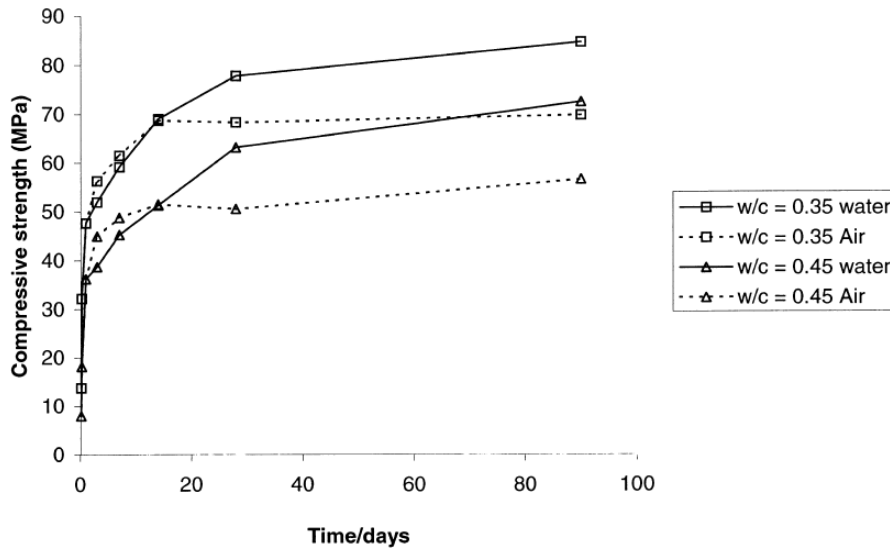


Figure 2.9: Compressive strength development of 1:1 ratio of CAC to GGBFS mixes cured at 20°C [12]

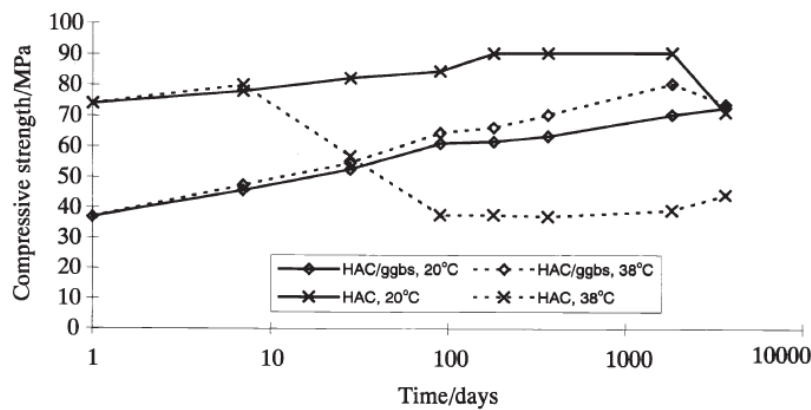


Figure 2.10: Compressive strength development of 50% CAC - 50% GGBFS blends up to ten years [13]

Singh et al. [13] also studied the compressive strength development of 50% CAC - 50% GGBFS blends up to ten years at 20°C and 40°C and the results related to that are portrayed in Figure 2.10 above. As seen in Figure 2.10, samples prepared with neat CAC experienced reduction in strength whereas slag incorporated mixes demonstrated little or no reduction in strength up to ten years.

### 2.7.2 CAC-Fly Ash Binary System

The use of combined system consisting of CAC and fly ash provides similar advantages to CAC-GGBFS combinations. The reactive silica found in fly ash facilitates the formation of stable gehlenite hydrate ( $C_2ASH_8$ ) and the decrease of strength seen in CACs are hindered this way. For this reason, the use of fly ash along with high alumina cements has been studied besides other pozzolanic materials having similar natures.

Pacewska et al. [14] investigated how the addition of different fly ashes affects the early hydration behavior of calcium aluminate cement. In this study, two different types of fly ashes are used which are namely pulverised fly ash and fluidized fly ash. Experiments are carried out using two different replacement ratios as 5% and 25% and the effects of addition of portland cement on calcium aluminate cement were also examined. The rate of heat evolution curves of pastes with the replacement of different additives are shown in Figure 2.11 below [14].

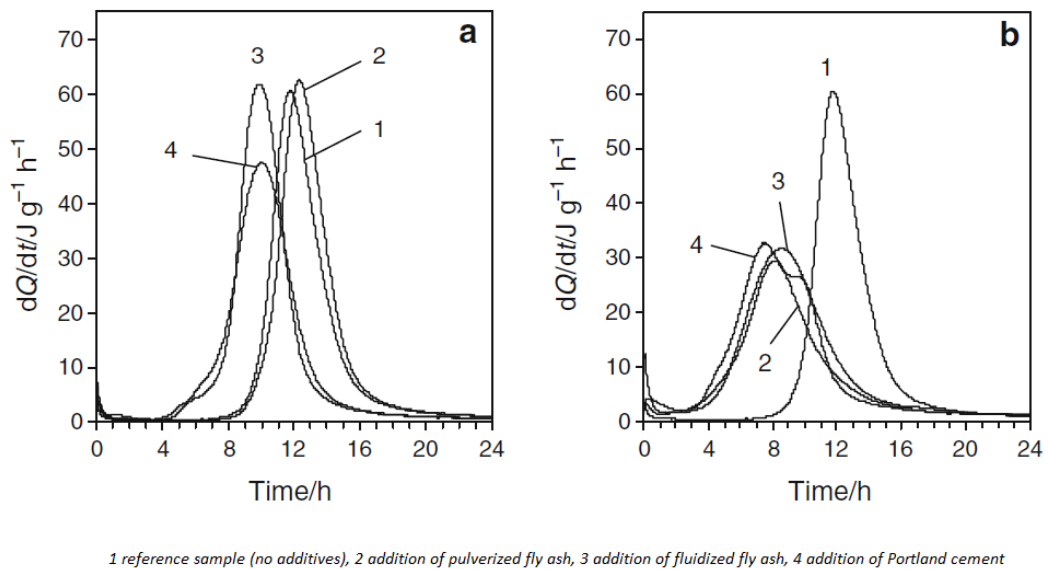


Figure 2.11: The rate of heat evolution curves of pastes with the replacement of different additives a) 5% of additive b) 25% of additive [14]

As it can be seen from Figure 2.11, addition of fluidized fly ash as a 5% replacement

accelerated the hydration process whereas pulverized fly ash did not create such an effect. On the other hand, 25% replacement of additives caused the accelerating effect without an exception. However, the intensities of main peaks displayed a lower trend which may be due to the lower initial activities of the additives [14].

Lopez-Zaldivar et al. studied the influence of the addition of municipal solid waste fly ashes on calcium aluminate cement. In order to get an understanding about the porosity of specimens which can be directly related to compressive strength, mercury intrusion porosimetry technique was utilized. Mortars with the same cement-aggregate ratio and having the same diameters were subjected to the porosity tests. As a result, mortars which include treated fly ash resulted as 32.64% less porous compared to the reference mortars consisting of plain CAC [5]. When these results are compared with the ultimate strength values, a direct proportionality between porosity results and strength values can be obtained. The following table summarizes the findings of this study [5].

Table 2.4: Properties of reference and TFA (Treated Fly Ash) mortars [5]

|                              | Reference mortar | TFA Mortar   |
|------------------------------|------------------|--------------|
| Capillary volume             | 55%              | 49%          |
| Porosity                     | 13.3484%         | 8.9907       |
| Specific surface             | 3834 $m^2/g$     | 3522 $m^2/g$ |
| 90 days compressive strength | 66.11 MPa        | 98.26 MPa    |
| 90 days bending strength     | 8.78 MPa         | 14.66 MPa    |

According to Collepari et al. [15], pozzolanic materials have the potential to create a mechanically stable system where strength reductions characteristic of high alumina cements are not seen. In that respect, two supplementary cementitious materials which are silica fume and fly ash were selected to be used. 20% replacement with fly ash showed reductions in strength at all temperatures except for 5°C where conversion of calcium aluminate hydrates is believed to occur at very late ages. On the other hand, 40% replacement resulted in rather close strength values at different temperatures and ages. The corresponding strength development curves of mortars prepared with the partial 20% and 40% replacement of fly ash are illustrated in Figures 2.12 and 2.13 respectively [15].



Collepari et al. also carried out XRD analysis for mortars containing 20 mass% fly ash at the curing age of 300 days and the relative patterns are shown in Figure 2.14 [15].

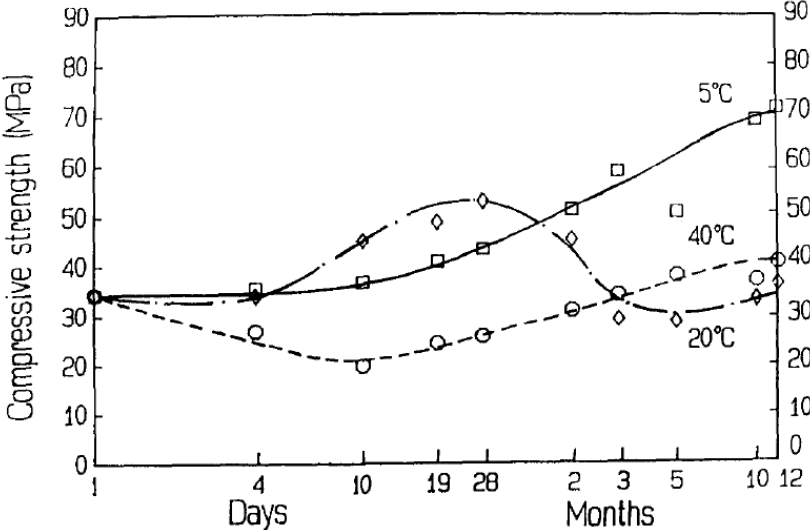


Figure 2.12: Strength development of mortars prepared with the partial 20% replacement of fly ash [15]

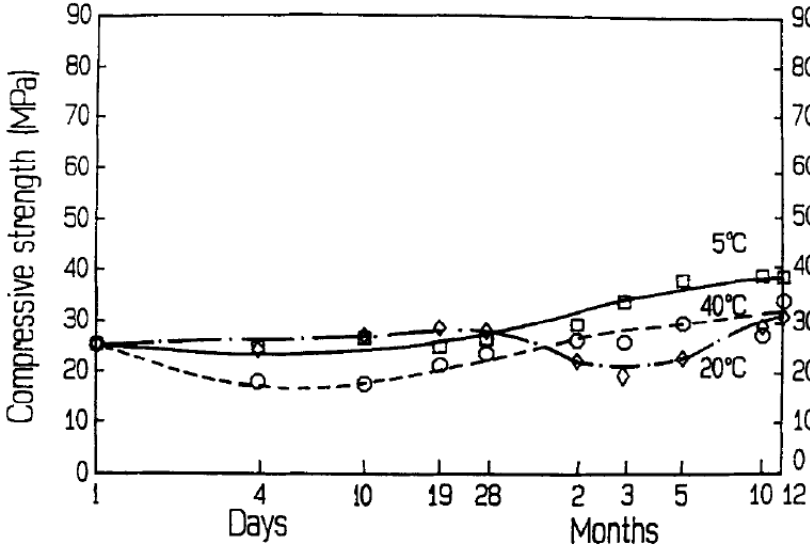


Figure 2.13: Strength development of mortars prepared with the partial 40% replacement of fly ash [15]

From Figure 2.14, it can be said that straeltingite peaks are weak comparatively. Thus, the fly ash used did not seem to provide sufficient silica that can trigger the formation of stable straeltingite particularly at a replacement level of 20%.

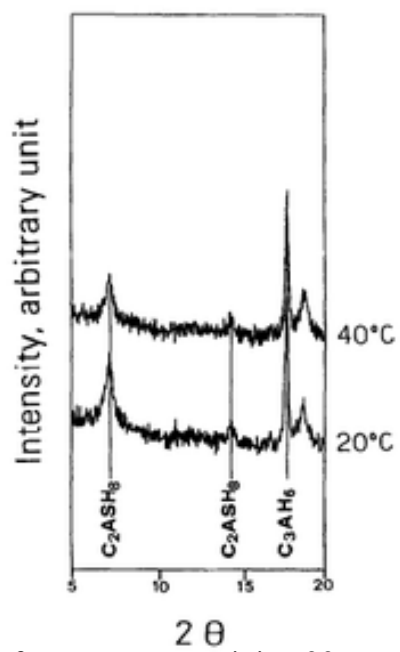


Figure 2.14: XRD analysis for mortars containing 20 mass% fly ash at the curing age of 300 days [15]

## **CHAPTER 3**

### **EXPERIMENTAL STUDY**

#### **3.1 General**

The use of calcium aluminate cement as a sole binder has been reported to be problematic over the past few decades due to strength reductions in the long-term use. For this reason, this study was intended to observe the changes that may possibly occur in the strength development and hydration of calcium aluminate cements by incorporating mineral admixtures. To investigate compressive strength and microstructural development of blended cements, two different supplementary cementitious materials (fly ash and GGBFS) were selected. Then these supplementary cementitious materials were used in different amounts together with CAC to prepare pastes and mortars to be tested. Fly ash was used 10,20 and 30% (by mass) and GGBFS was used 20,40 and 60% (by mass) to replace CAC. By using these materials, chemical, physical and mineralogical analyses were applied on a total of 7 different mixes. All the tests were done in Middle East Technical University Materials of Construction Laboratory.

#### **3.2 Materials**

Three different materials which are CAC, fly ash and GGBFS were used during this study. All materials were provided by ÇimSA Cement Production and Trade Company. Oxide and mineralogical compositions of those materials are presented in the sections labelled as 3.2.1 and 3.2.2.

### 3.2.1 Mineralogical Composition

The mineralogical compositions of all materials used in this study were found out with the aid of X-Ray Diffraction (XRD) analysis. These analyses were done with BTX-475 Benchtop X-Ray Diffractometer equipment. XRD patterns of samples were obtained using Cu radiation of 40kV/3mA and the range covers 5 to 55  $2\theta$ . The related XRD patterns of CAC, GGBFS and fly ash are illustrated in Figures 3.1,3.2,3.3 in sequence.

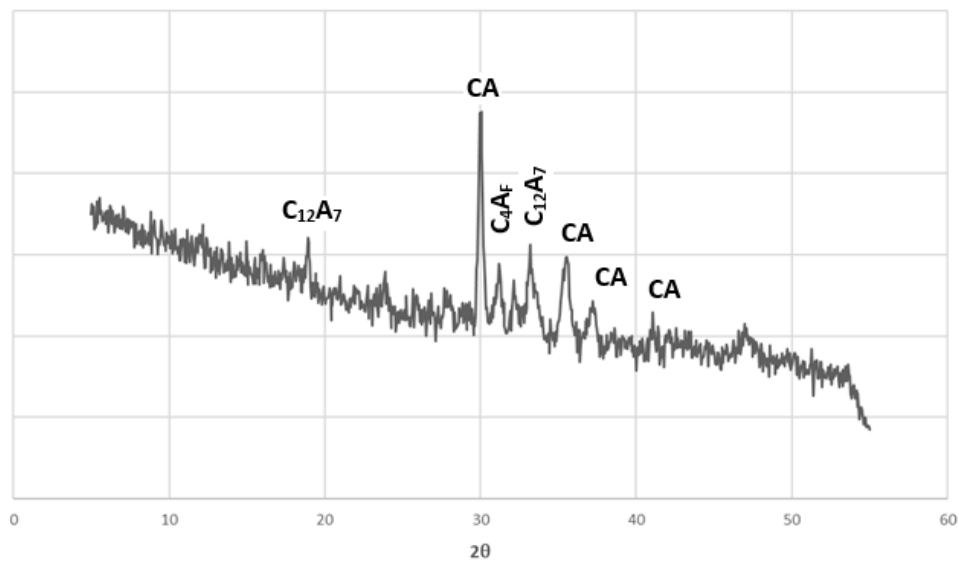


Figure 3.1: XRD Pattern of CAC

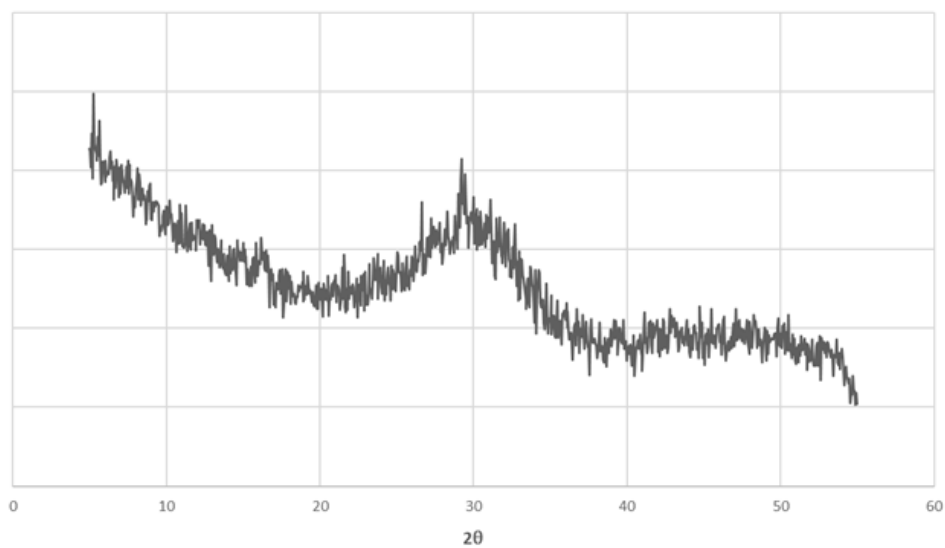


Figure 3.2: XRD Pattern of GGBFS

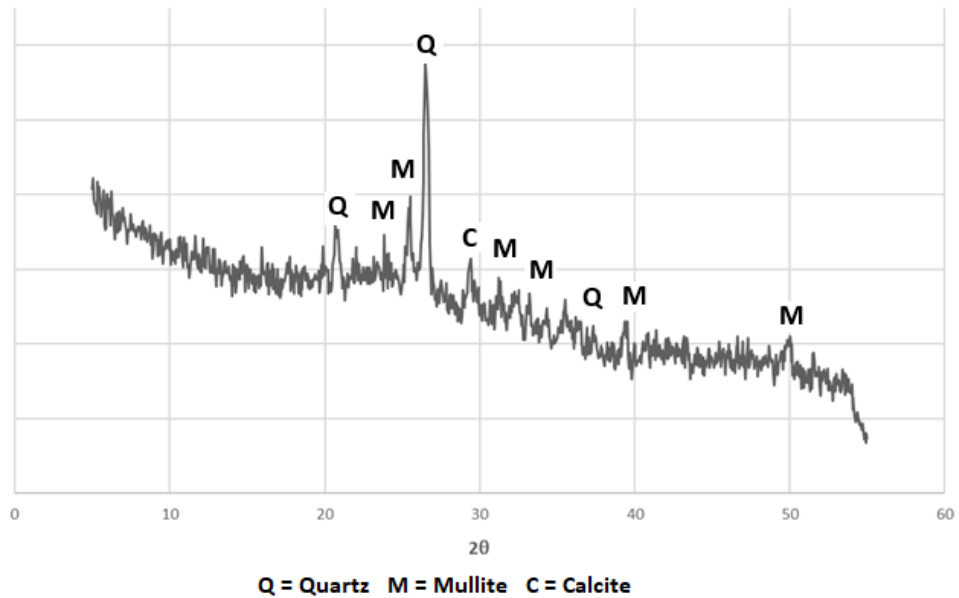


Figure 3.3: XRD Pattern of Fly Ash

As seen in Figure 3.1, CAC is composed of mainly  $CA$ ,  $C_{12}A_7$  and  $C_4AF$ . Among those, the amount of  $CA$  dominates the mineralogical composition of CAC expectedly as it is the chief unhydrated phase in almost all high alumina cements. On the other hand, identification of phases in the XRD pattern of GGBFS is not very possible as it displays a glassy amorphous structure thus, the crystalline phases could not be detected. As opposed to GGBFS, phases in fly ash are more clear and identified as seen in Figure 3.3. Quartz and mullite are the dominating phases together with some amount of calcite.

### 3.2.2 Chemical Composition

Oxide compositions of three materials used in this study were determined by X-Ray fluorescence (XRF) analysis. The results are shown in Table 3.1

Table 3.1: Chemical Compositions of Materials

| Oxides (%)                         | CAC  | GGBFS | Fly Ash |
|------------------------------------|------|-------|---------|
| <i>CaO</i>                         | 35.0 | 36.9  | 14.12   |
| <i>SiO<sub>2</sub></i>             | 4.02 | 33.5  | 44.59   |
| <i>Al<sub>2</sub>O<sub>3</sub></i> | 37.1 | 11.8  | 21.94   |
| <i>Fe<sub>2</sub>O<sub>3</sub></i> | 15.9 | 0.98  | 6.73    |
| <i>TiO<sub>2</sub></i>             | 2.07 | 0.67  | 0.72    |
| <i>MgO</i>                         | 0.73 | 5.98  | 2.95    |
| <i>SO<sub>3</sub></i>              | 0.05 | 1.43  | 5.43    |
| <i>K<sub>2</sub>O</i>              | 0.14 | 0.84  | 1.91    |
| <i>Na<sub>2</sub>O</i>             | 0    | 0.29  | 1.01    |

### 3.2.3 Density of Materials

Densities of materials used in this study were determined according to ASTM C188. The standard Le Chatelier Flask was utilized and kerosene was used for density determination. Displaced volumes were recorded when a certain time passed after the cement or mineral admixtures were introduced. In accordance with these, densities were calculated using the expression given below;

$$\rho(g/cm^3) = \text{mass of cement}(g) / \text{displaced volume}(cm^3) \quad (3.1)$$

Consequently, the densities found in that way are shown in Table 3.2.

Table 3.2: Densities of materials

| Name of the binder | Density ( $g/cm^3$ ) |
|--------------------|----------------------|
| CAC                | 3.3                  |
| GGBFS              | 2.87                 |
| Fly Ash            | 2.34                 |

### 3.2.4 Fineness of Materials

Fineness values were determined according to ASTM C204. Testing was done using the Blaine air permeability apparatus. During the test, a certain amount of air was

drawn through a bed of cement whose porosity is known. The specific surface of test samples are found according to the expression given in ASTM C204 [27]. As a result, fineness values of the materials were calculated and given below.

Table 3.3: Fineness of materials

| Name of the binder | Specific Surface Area ( $cm^2/g$ ) |
|--------------------|------------------------------------|
| CAC                | 4400                               |
| GGBFS              | 4300                               |
| Fly Ash            | 4780                               |

### 3.3 Mix Types and Mixing Protocols

#### 3.3.1 Mix Types

In this study, calcium aluminate cement was used as the main binder and it was blended with either GGBFS or fly ash. A total of 7 mixtures were prepared and subjected to different analyses. Table 3.4 shows mixture designations according to the materials used and their proportions.

Table 3.4: Mixture designations

| Mix Type | Proportions of the mixtures |
|----------|-----------------------------|
| C        | 100% C                      |
| S20      | 80% C + 20% GGBFS           |
| S40      | 60% C + 40% GGBFS           |
| S60      | 40% C + 60% GGBFS           |
| F10      | 90% C + 10% FA              |
| F20      | 80% C + 20% FA              |
| F30      | 70% C + 30% FA              |

#### 3.3.2 Mixture Preparation

For the analyses carried out in this study either pastes or mortars were prepared and tested. The mortars were prepared in accordance with TS EN196-1 where a constant water to cement ratio of 0.5 is prescribed. To prepare mortars, 1350 g of sand, 450 g of

binder and 225 g of water were mixed regardless of the binder types and proportions. After the mixing, for compressive strength tests, mortars were filled into prismatic molds whose dimensions are 40x40x160 mms. To prepare pastes, first binders in the powder form were mixed using the standard mixer specified in TS EN 196-1 at a rotational speed of  $140 \pm 5 \text{min}^{-1}$  for a minute then mixed at  $285 \pm 10 \text{min}^{-1}$  for 45 seconds. As a result of this, homogenous binder combinations were obtained and this process was also repeated in the preparation of mortars. Water to cement ratio of 0.5 was the same for the blended cement pastes. All mortars and pastes were stored in water and placed into the humidity cabinets operated at related temperatures.

### **3.4 Tests and Analyses Performed**

The tests and analyses done in this study were grouped into two as: 1)Analyses performed on cement pastes 2)Tests performed on cement mortars.

#### **3.4.1 Analyses performed on cement pastes**

X-Ray Diffraction and heat of hydration analyses were carried out in cement pastes.

##### **3.4.1.1 Heat of Hydration**

There are basically three methods to measure the heat of hydration which can be enumerated as isothermal conduction calorimetry method, adiabatic and semi-adiabatic method and heat of solution method. In a study carried out by Sanderson et al., the results of isothermal calorimetry and semi-adiabatic calorimetry were compared with each other and a positive correlation was obtained [28]. However, it was pointed out that isothermal calorimetry method is advantageous compared to semi-adiabatic method in terms of sample size and instrument stability [28]. Isothermal conduction calorimetry method is solely utilized in this study.

During the experiment, heat flow from the sample is tracked by isothermal conduction calorimetry while the sample and the surroundings are maintained at a constant



temperature. Then the heat of hydration can be directly obtained as the heat flow from the reference material is compared with the heat flow from the sample. Tam air isothermal calorimetry was specifically used for the isothermal conduction calorimetry method in this study. In Tam air isothermal calorimetry, channels labeled with B show reference channels whereas A is for test samples. The calorimetry has 8 channels in total and 8 different samples can be tested at the same time. Cement pastes are placed in 20 ml glass ampoules and the same ampoules can also be used for the reference samples. Further information about calorimeter can be obtained from TAM Air Calorimeter Operator's Manual [29].

Before testing, the required amount of materials was calculated as test and reference samples which should have the same heat capacity values. As a result, 10.1 grams of pastes were prepared for each mix and the water-cement ratio was held at 0.5. All pastes were stirred without delay with the help of a metal rod. Then, the prepared pastes were placed in 20 ml glass ampoules. To start the test, detailed data about the experiment were provided and the stirred test samples were placed to the channels labeled with B. During the experiment, the rate of heat generated with respect to time is recorded by the isothermal calorimetry. Afterwards, in order to find the total heat of hydration, the area under the heat evolution curve with respect to time is summed or in other words, the integral of heat flow computed gives the total heat of hydration. This process was repeated for three temperatures which are 20°C, 40°C, 60°C and each of them was tested for 24 hours.

#### **3.4.1.2 X-Ray Diffraction Analyses**

X-Ray Diffraction (XRD) method is a well-known and accurate method used to find out the crystal structure of cement pastes. For all XRD analyses, BTX-475 Benchtop XRD System was used to reveal the microstructure of hydrated cement pastes. Samples were scanned from 5 to 55  $2\theta$  using Cu radiation. Pastes that were intended to be subjected to XRD analyses were cured in their closed molds at related temperatures. When the testing date arrived, they were pulverized so that the particles can pass a 100  $\mu\text{m}$  sieve. To identify crystal phases, X'Pert High Score software and the information in the related literature were used together [30].

### **3.4.2 Compressive strength tests of cement mortars**

Compressive strength tests were carried out according to TS EN196-1 [31]. Testing ages were 1,3,7,14,28,56,90 and 180 days for all mixes. As the standard prescribes, a constant water-cement ratio of 0.5 was used. Mortar specimens were casted into prismatic molds that have dimensions of 4x4x16 cm. During the preparation of mortar, standard sand and distilled water were used and sand-cement ratio was 3 for all mixes. After a period of 24 hours after casting, demoulding takes place and the demoulded mortars were placed in a moist room or moist cabinets at relevant temperatures. At the testing age, mortars were initially broken into halves as they were subjected to the bending test and these samples were then subjected to compressive force acting at nominal dimensions of 40x40 mm. Then the resulting forces were divided by the related area  $1600 \text{ mm}^2$  to obtain the compressive strength value.

## **CHAPTER 4**

### **RESULTS AND DISCUSSION**

#### **4.1 Effect of Temperature on Plain CAC**

The following sections are intended to investigate the effect of temperature on heat of hydration, compressive strength and microstructural development of plain CAC samples throughout the testing period.

##### **4.1.1 Effect on Heat of Hydration**

The rate of heat evolution curve of the plain CAC pastes cured at 20°C, 40°C and 60°C obtained using isothermal calorimetry are shown in Figure 4.1 with respect to the corresponding curing temperature. The heat of hydration values are examined up to 24 hours by using this method.

When early heat evolution characteristics of CAC pastes at different temperatures given in Figure 4.1 was examined, it was observed that rate of heat of hydration and heat of hydration curves of CAC paste at 60°C were completely different than those at 20°C and 40°C. There appears to be a dormant period in the latter which indicates an extremely slow rate of reaction. This period is about 5h at 20°C whereas at 40°C, it is reduced to about 3h. This shortening may be due to increased reactivity at higher temperature. On the other hand, either no such dormant period exists or it is extremely shortened so that it could not be observed at 60°C.

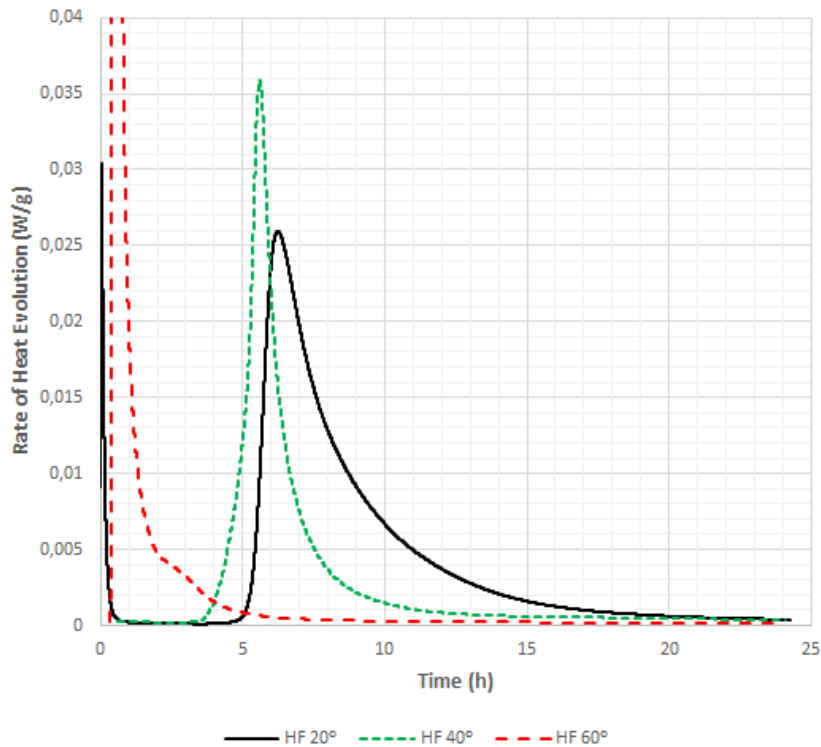


Figure 4.1: Rate of Heat Evolution of Plain CAC at Three Different Curing Temperatures

As seen in Figure 4.1, the rate of heat evolution is proportional to the curing temperature and in that respect, as the curing temperature rises the rate of heat evolution increases as well. This effect is more clear in the pastes cured at 60°C as the rate of heat evolution dramatically increased at this temperature. A peak in the rate of heat evolution curve of pastes cured at 20°C was experienced at about 6 hours whereas this value was at about 5 hours at 40°C and about half an hour at 60°C. Thus, from here the conclusion that hydration progresses more rapidly at elevated temperatures can be derived.

#### 4.1.2 Effect on Compressive Strength Development

With the aim of observing the compressive strength development of plain CAC at different curing temperatures, whose results are used as a control group, compressive strength tests are applied at certain ages up to 180 days and the corresponding results are summarized in Table 4.1. Average compressive strength values were obtained

by taking the average of six tested specimens. In addition to that, to express how compressive strength development occurred in a visual way, the graph seen in Figure 4.2 is presented.

Table 4.1: Compressive Strength Values of Plain CAC Cured at 20, 40, 60°C (MPa)

|      | 1 day | 3 days | 7 days | 14 days | 28 days | 56 days | 90 days | 180 days |
|------|-------|--------|--------|---------|---------|---------|---------|----------|
| 20°C | 54.5  | 54.4   | 70.0   | 67.6    | 63.4    | 58.0    | 41.1    | 38.6     |
| 40°C | 33.3  | 22.0   | 24.0   | 22.6    | 26.4    | 27.3    | 31.8    | 27.6     |
| 60°C | 25.1  | 25.0   | 26.1   | 25.8    | 25.4    | 25.9    | 27.2    | 30.2     |

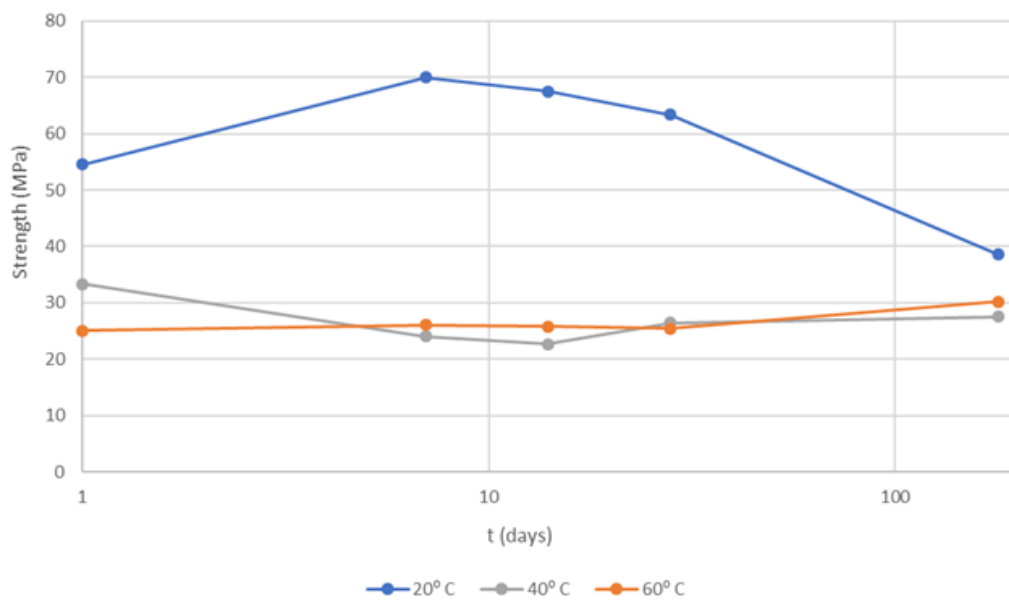


Figure 4.2: Compressive Strength Development of Plain CAC at Three Different Curing Temperatures

When test results obtained at 20°C are investigated, the increase in compressive strength values seem to continue up to 7 days and afterwards a gradual decrease is observed. On the other hand, consideration paid to the compressive strength development from 1 day till 180 days, the peak value corresponds to the obtained strength at the age of 7-day testing. After a period of 7 days-long curing time, the decline in compressive strength values constantly progresses up to 180 days and the fact that compressive strength at 180 days is approximately 45% less than the maximum value

attained at 7 days can be observed by delving into the results presented. At this point, the conclusion indicating the conversion process started after 7 days of curing time may well be reached. In section 4.1.3, this conclusion will be emphasized with the aid of the results of X-Ray diffraction studies.

As the compressive strength development at 40°C is examined, the decline in compressive strength values seem to exist at 3 days of continuous moist curing. As the temperature is enhanced, the conversion process speeds up and compared to the descending trend observed after 7 days at 20°C curing, this case can be monitored starting from 3 days at 40°C curing temperature. This effect confirms the statements temperature and the rate of conversion is directly proportional expressed in the literature. [8, 32, 17, 25, 33, 34] Apart from these, handling the whole development process displays the greatest compressive strength value belonging to the strength value attained at 1 day. From this point on, despite the fact that strength values showcase slight fluctuations, there does not seem to be any notable changes.

When test results obtained at 60°C are investigated, a case of conversion process does not seem to exist. The hydration process at 60°C happens a lot faster in proportion to the other curing temperatures and as a result of this, hydration occurred in 1 day to a large extent causes almost the ultimate strength value that can be achieved in that amount of curing temperature. Having said that going over the rate of heat evolution curve given in Figure 4.1 proves how rapid the hydration process progresses and this is a reflection of the above-mentioned statement. In the ongoing process, from 56 days strength value to the one attained on 180 days a slight increase takes place.

It is known that the two metastable hydration products ( $CAH_{10}$  and  $C_2AH_8$ ) of CAC result in high early strength due to their low densities (1.7 and 1.9  $g/cm^3$ , respectively). These low-density products form rapidly and fill the pores, leading to high strength. Upon their conversion however, porosity increases and consequently strength decreases. Formation of  $C_3AH_6$ , which has a density of 2.5  $g/cm^3$ , causes the increased porosity. Furthermore, considerable amount of water is released by the conversion which also plays a major role of increase in porosity. Therefore, early rapid formation of the stable hydrate,  $C_3AH_6$  directly, at high temperatures, although it reduces the early strength, will not result in further reduction in strength with time.

Indeed, when 1-day and 180-days strengths of CAC mortars cured at 20°C, 40°C, and 60°C are compared, it can be said that as the curing temperature increases, 1-day strength reduces as shown in Figure 4.3. 1-day strength of CAC mortars cured at 60°C was almost 50% lower than that cured at 20°C. On the other hand, almost 30% strength reduction was experienced in 20°C-cured mortars whereas 20% strength increase was attained in 60°C-cured mortars, after 180 days. Thus, it can be stated that facilitating the rapid formation of  $C_3AH_6$  in CAC hydration by early high temperature application may have the possibility of being used beneficially for preventing later age strength reduction due to the conversion of the metastable hydration products.

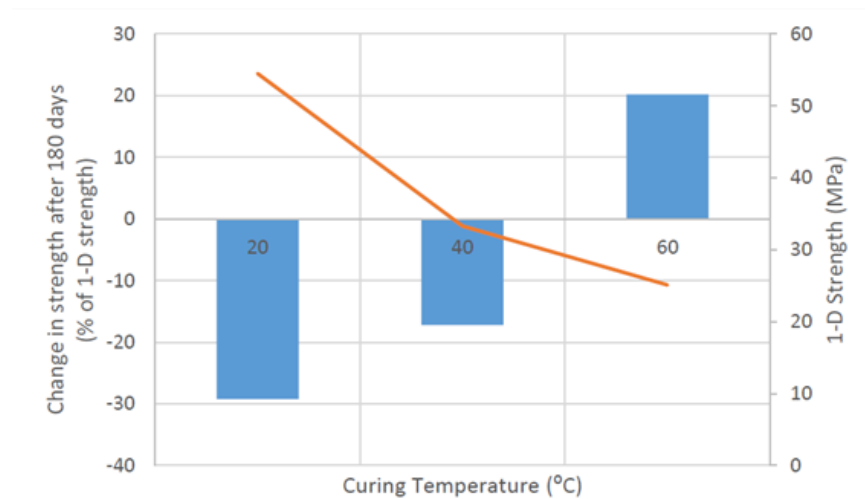


Figure 4.3: 1-day strength and change in strength at 180 days at different curing temperatures

#### 4.1.3 Effect on Microstructural Development

XRD studies were carried out to see the microstructural development of plain CAC pastes and to find out the phases at certain stages that may possibly triggered the compressive strength trends revealed in section 4.1.2. The results of the analyses are portrayed in Figures 4.4 - 4.6.

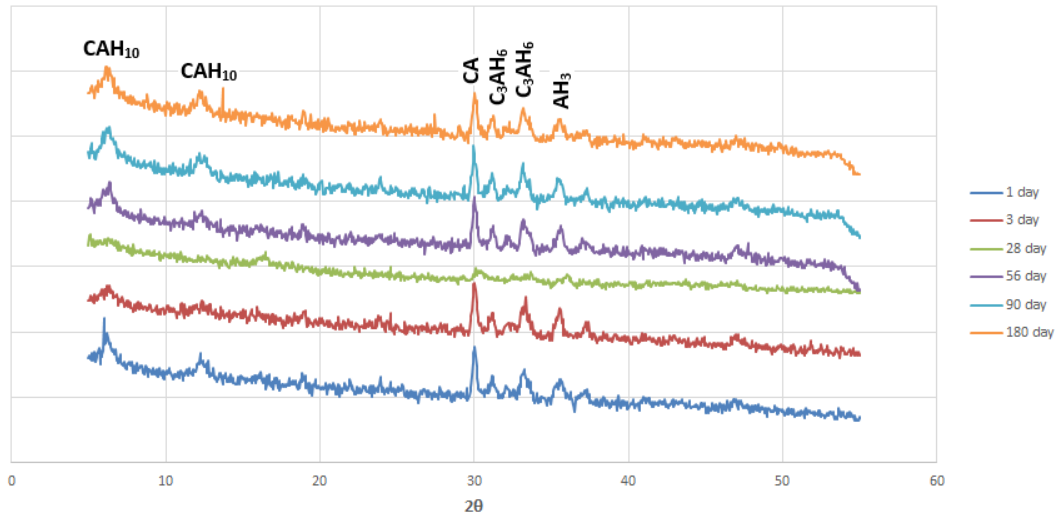


Figure 4.4: XRD Patterns of plain CAC pastes cured at 20°C

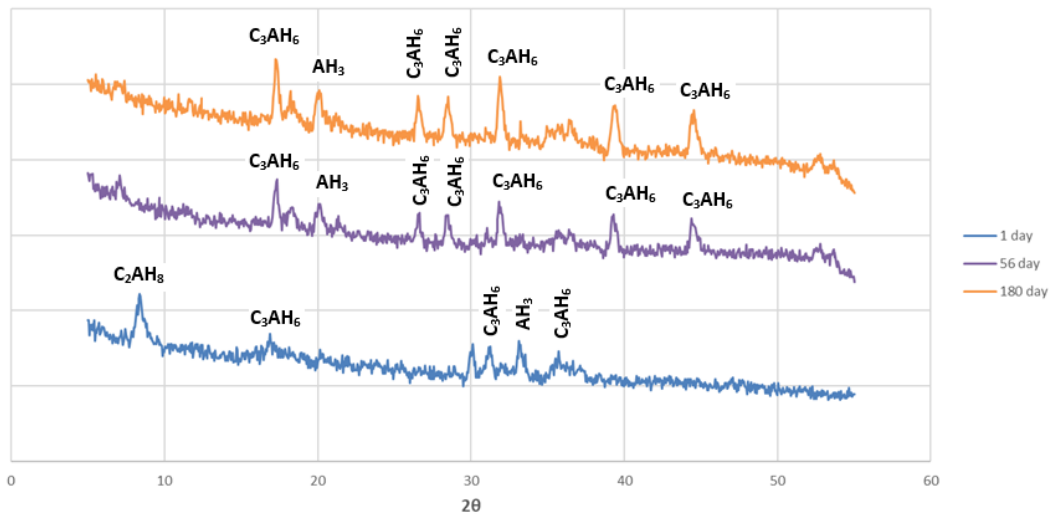


Figure 4.5: XRD Patterns of plain CAC pastes cured at 40°C



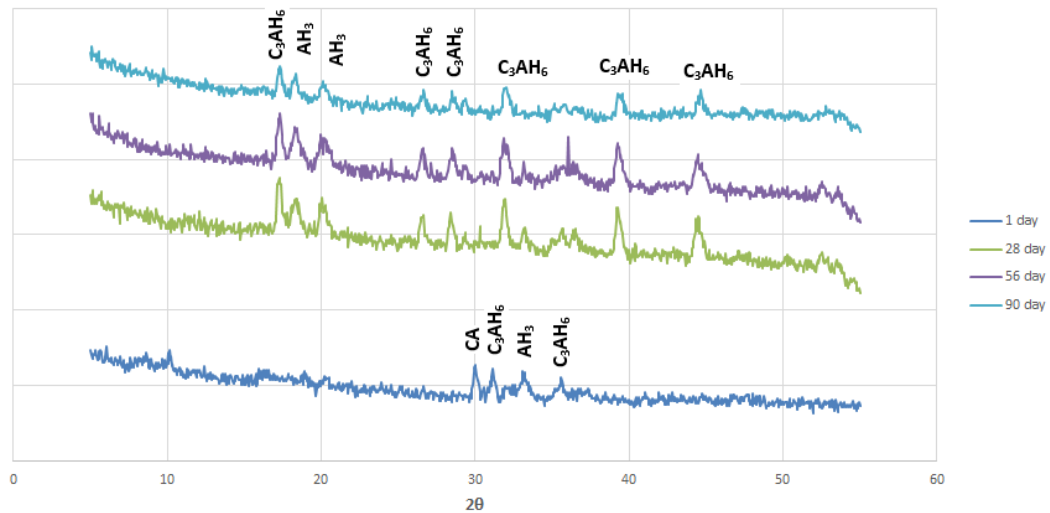


Figure 4.6: XRD Patterns of plain CAC pastes cured at 60°C

As it can be seen from Figure 4.4, the phases found using the X-Ray Diffraction technique do not show a great deal of variation as the curing time for pastes change. However, one significant observation to touch on is that at the first day, the intensity of  $CAH_{10}$  peaks are somewhat larger but on the following stages, especially at 3 and 28 days curing, those peaks seem to almost disappear. The following three curing stages boost the formation of  $CAH_{10}$  again nonetheless, their intensities are not as high as the ones observed at 1 day. This can explain the decline happened in the strength development of plain CAC mortars cured at 20°C. The formation of  $C_3AH_6$  begins at the 1st day and the intensities of  $C_3AH_6$  peaks have a tendency to increase up to 180 days except for an amorphous structure appeared at 28 days. In that respect, it can be implied that the formation of  $C_3AH_6$  starts directly at the very beginning and with the conversion of metastable products its existence does not cease, in fact increases, until the last testing age at 180 days. Therefore, these results prove the argument put forward in a bunch of sources in literature that complete conversion may take years to finalize particularly at low temperatures. [17, 35, 15, 14, 7]

When the results at 40°C are delved into, the  $C_2AH_8$  peak seen on the 1st day disappears at the later ages. Rather than the existence of  $C_2AH_8$ , new peaks labeled as  $C_3AH_6$  and  $AH_3$  form at the later ages whose are the products of the conversion reactions of calcium aluminates. To put it another way, stable hydration product

$C_3AH_6$  possessing a higher density value substitute the metastable product  $C_2AH_8$ . At the last testing age, namely 180 days, the characteristic peaks at 56 days remain the same however, their intensities are slightly greater compared to the former curing age. This is an indication of conversion being mostly completed. Moreover, compressive strengths at the age of 56 days and 180 days are almost the same which can also be attributed to the similar microstructures observed at these ages.

At 60°C metastable products are not observed throughout the entire testing ages. When this observation and compressive strength results are evaluated together it is clear that stable products seen starting from 1st day till the end reflect the steady trend of strength values. In fact,  $C_3AH_6$  formation starts immediately as the hydration takes place and strength results are not notably affected at later stages due to the precipitation of stable  $C_3AH_6$  and  $AH_3$ .

Considering the temperature-sensitivity of CAC hydration pointed out by Scrivener and Capmas [4], the XRD traces of CAC pastes cured at 20°C, 40°C, and 60°C were compared with each other after a hydration period of 1 day, as shown in Figure 4.7. As it can be seen in the figure,  $CAH_{10}$  was the main hydration product at 20°C. However, at 40°C, besides  $CAH_{10}$ ,  $C_2AH_8$  was also present. Part of these phases seemed to convert into  $C_3AH_6$  within as early as 1 day additionally,  $AH_3$  was observed too, as the possible sign of the conversion.

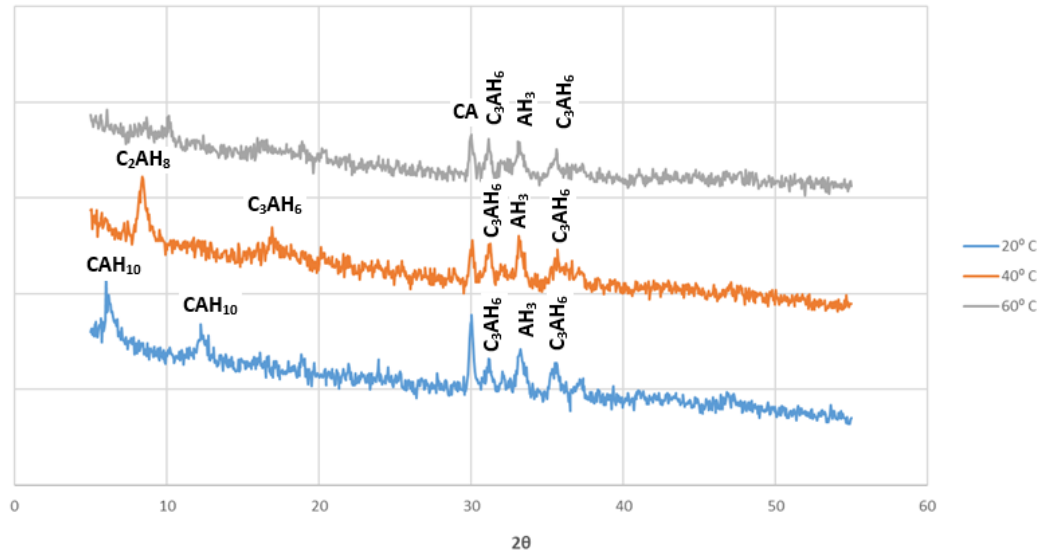


Figure 4.7: XRD patterns of CAC samples hydrated for 1 day at 20°C, 40°C, and 60°C

To summarize, the rates of conversion reactions depend on several factors such as moisture state, water content, and temperature [4]. Since the first two factors were constant, temperature effect was the only factor in this study. Although  $C_2AH_8$  was not present at 20°C, it appeared in the XRD of 40°C and  $C_3AH_6$  was also observed at 40°C hydration. Therefore, conversion of  $C_2AH_8$  into  $C_3AH_6$  occurred in this case. On the other hand,  $C_3AH_6$  was the only hydration product, besides  $AH_3$  which is not significant, at 60°C. Thus, it can be stated that at high temperatures, 60°C in this case,  $C_3AH_6$  forms directly as a result of the hydration of  $CA$  without any conversion reaction.

## 4.2 Effect of Temperature on CAC Blends

### 4.2.1 Effect on Heat of Hydration

The rate of heat evolution curves of the CAC blended pastes cured at 20, 40 and 60°C obtained using isothermal calorimetry are shown in Figures 4.8, 4.9, 4.10, 4.11, 4.12, 4.13 with respect to the type of mineral admixture incorporated and up to 24 hours of

curing age. The rate of heat of hydration curves of the cements at 20°C, for the first 24 hours are shown in Figures 4.8, 4.9. Various important features of these curves may be listed as:

- a. There is a dormant period in all cases. Slag incorporation does not affect the length of this period significantly. On the other hand, fly ash incorporation results in shortened dormant periods. This may be attributed to the accelerating effect of fly ash particles due to their higher fineness. As having 4780  $cm^2/g$  of Blaine fineness value, fly ash is the finest material among all that were used. This effect is more pronounced for 20% and 30% fly ash incorporations.
- b. The second peak in the graph corresponds mainly to  $CAH_{10}$  formation. There occur around 58%, 69%, and 81% decrease in the height of this second peak for 20%, 40%, and 60% CAC replacement by slag. There is a linear relationship between the decrease in rate of heat of hydration and the amount of slag used as illustrated in Figure 4.8. The  $CAH_{10}$  peak is reduced by fly ash use, also. However, it was not possible to find a relationship between fly ash amount and the reduction in the height of the peak. The average amount of reduction is about 50% in the case of fly ash incorporation.
- c. Rate of heat flow is slowed down by slag or fly ash use as can be seen from the slopes of the acceleration periods in Figure 4.10. Reduction in rate is almost constant for fly ash-incorporated pastes whereas it increases with the amount of slag in slag-incorporated pastes.

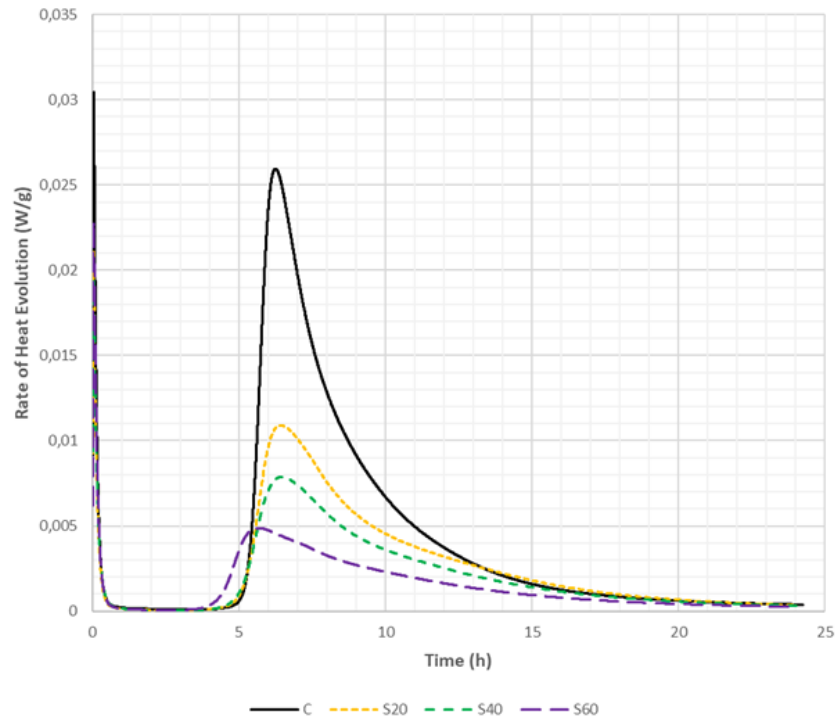


Figure 4.8: Rate of Heat Evolution of CAC-GGBFS mixes cured at 20°C

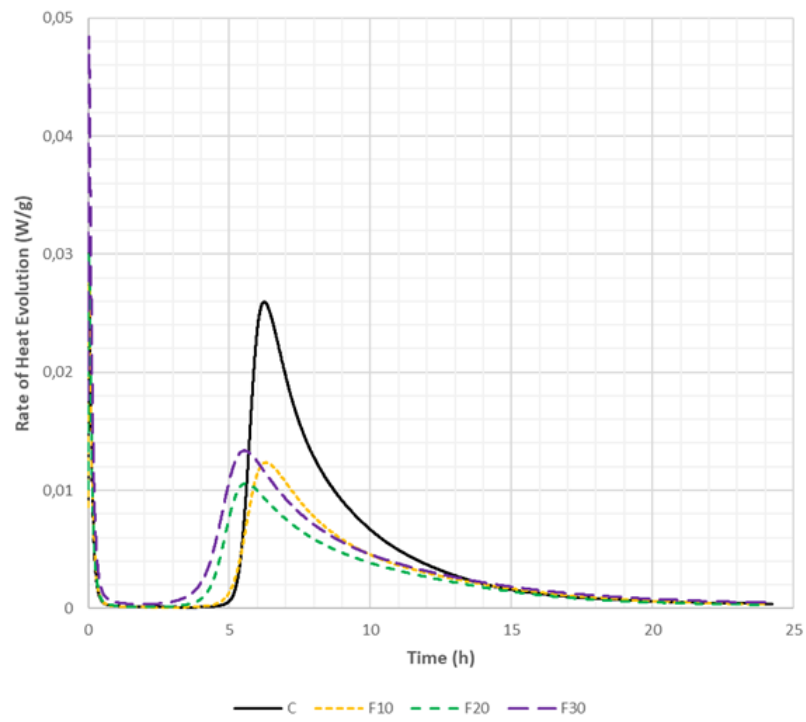


Figure 4.9: Rate of Heat Evolution of CAC-FA mixes cured at 20°C

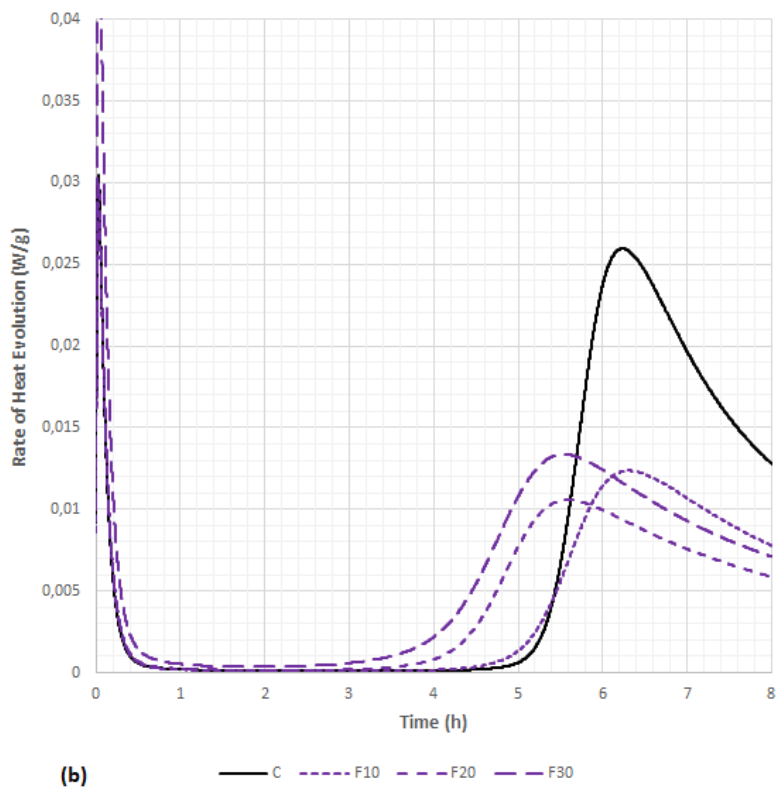
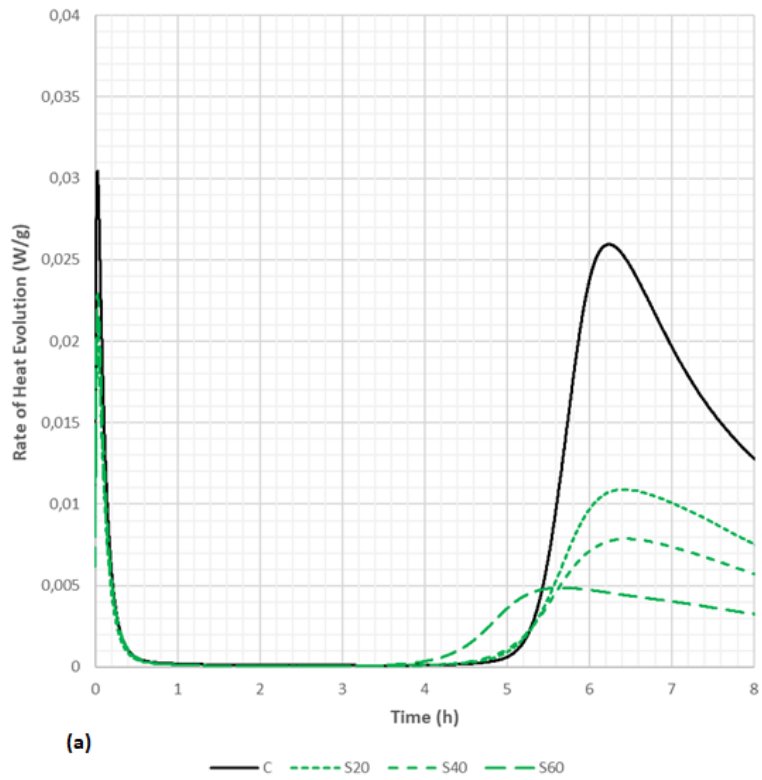


Figure 4.10: Comparative rates of heat flow in acceleration stage for (a) slag-incorporated and (b) fly ash-incorporated pastes cured at 20°C

The rate of heat of hydration curves of the blended cements at 40°C, for 24 hours are shown in Figure 4.11 and Figure 4.12 illustrates the rate of heat evolved during the first 7 hours. As it can be seen from Figure 4.11, the presence of slag strongly influences the intensities of main exothermic peaks, even a replacement ratio of 20 mass% slag causes a reduction in the peak value about 60%. Furthermore, replacing the CAC partially by either GGBFS or fly ash shortens the dormant period notably. This effect can be stated more easily for the blends that contain 30% or more from either mineral admixture.

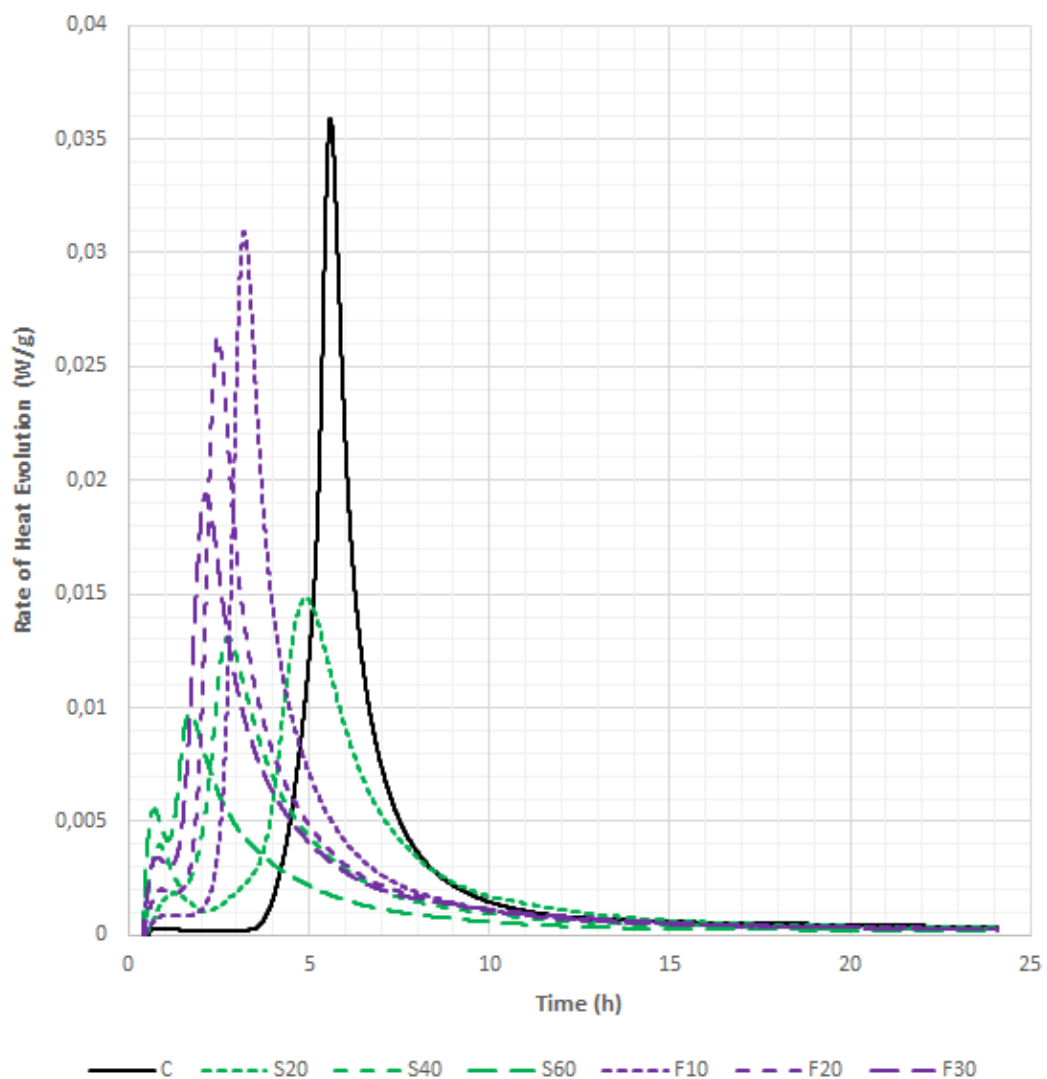


Figure 4.11: Rate of Heat Evolution of CAC-GGBFS and CAC-FA mixes cured at 40°C

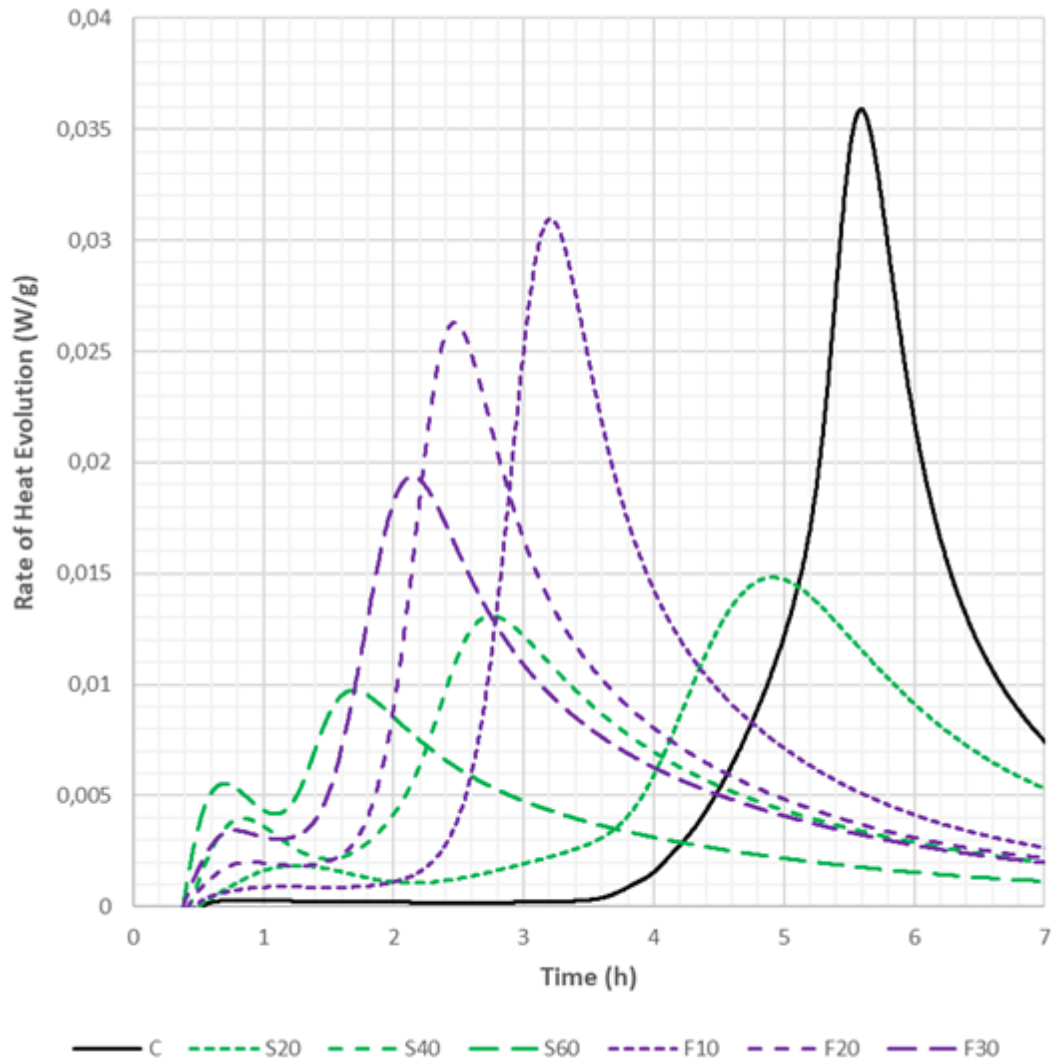


Figure 4.12: Rate of Heat Evolution of CAC-GGBFS and CAC-FA mixes cured at 40°C during the acceleration stage

The rate of heat of hydration of pastes cured at 60°C show uniquely rapid progress and because of that heat evolution curves of them are limited to 1 hour to identify the stages of the hydration in a more clear fashion. After that steady state stage takes place where diffusion control occurs. Related curve is presented in Figure 4.13. The sole effect seen with the presence of mineral admixtures at 60°C is that they decrease the rate of heat of hydration in association with the amount of mineral admixture used except for the mix labeled as S20.



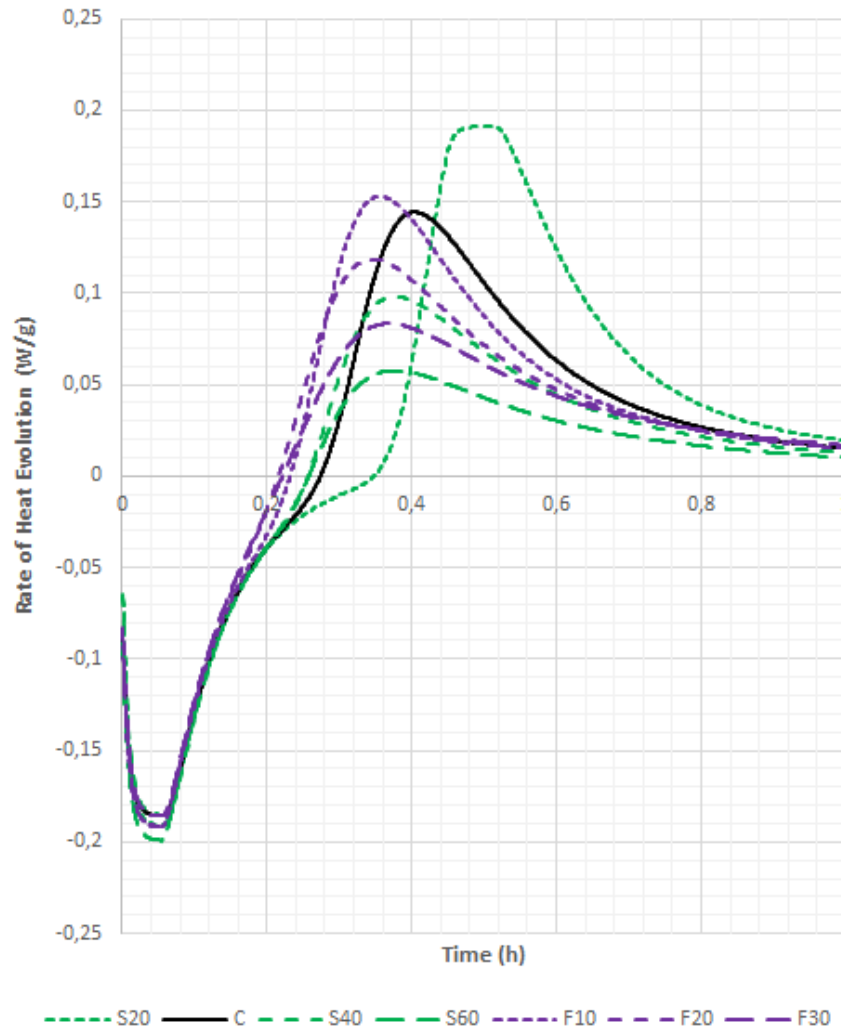


Figure 4.13: Rate of Heat Evolution of CAC-GGBFS and CAC-FA mixes cured at 60°C

To sum it all up, one conclusion shared by all mixes and all curing temperatures is that as the CAC amount gets less, the main peaks appear at lower values as can be seen in Figures 4.8, 4.9, 4.10, 4.11, 4.12, 4.13. At the curing temperature of 20°C, both GGBFS and fly ash incorporation decrease the rate of heat evolution of CAC but no significant delay in the main peaks can be observed. The decreasing rate of heat evolution can be explained with the slow hydrating nature of straeltingite originated from the silicates existing in both GGBFS and fly ash [15, 12, 13]. However, at 40°C curing period, incorporation of mineral admixtures brings about a remarkable delay in the appearance of main peaks along with a decreasing rate of heat evolution. The delay observed in the formation of main exothermic peaks can be attributed to the

less development of calcium aluminate hydrates. On the other hand, the hydration happens swiftly at the curing temperature of 60°C meaning it is not very likely to determine any delays however, a decrease in the rate of heat evolution depending on the amount of mineral admixture used is self-evident. All in all, it is fairly obvious that both CAC/GGBFS and CAC/FA ratios are critical for the hydration mechanism of CAC blends.

#### 4.2.2 Effect on Compressive Strength Development

To understand the effect of mineral admixture incorporation to CAC in terms of the compressive strength development, the mixes whose nomenclature stated in the section 3.3.1 were tested at the same testing ages applied for plain CAC without admixture. The results obtained are shown in Tables 4.2,4.3,4.4 for different curing temperatures. Additionally, to visually examine the data, the compressive strength values are plotted against time and presented in Figures 4.14 - 4.19.

Table 4.2: Compressive Strength Values of Plain CAC and CAC Blend Mixes Cured at 20°C (MPa)

|     | 1 day | 3 days | 7 days | 14 days | 28 days | 56 days | 90 days | 180 days |
|-----|-------|--------|--------|---------|---------|---------|---------|----------|
| C   | 54.5  | 54.4   | 70.0   | 67.6    | 63.4    | 58.0    | 41.1    | 38.6     |
| S20 | 41.4  | 51.3   | 58.9   | 59.9    | 59.2    | 50.1    | 49.1    | 46.4     |
| S40 | 30.7  | 36.2   | 42.6   | 42.6    | 46.5    | 48.5    | 39.4    | 42.5     |
| S60 | 14.2  | 16.7   | 19.5   | 21.3    | 28.2    | 32.0    | 23.8    | 27.2     |
| F10 | 43.6  | 53.9   | 56.4   | 61.6    | 56.2    | 44.6    | 51.8    | 49.4     |
| F20 | 36.4  | 45.8   | 49.7   | 54.2    | 46.5    | 40.0    | 44.4    | 45.9     |
| F30 | 29.0  | 35.4   | 39.5   | 42.8    | 38.8    | 32.8    | 41.0    | 39.3     |

When the compressive strength values of plain CAC and GGBFS incorporated mixes continuously cured at 20°C are compared with one another, one mutual outcome for all GGBFS incorporated mixes that can be reached is all of them seem to have more strength values in the long term relative to neat CAC mortars. Compressive strength values of mixes that contain 20 mass% GGBFS have a tendency to increase up to 28 days however, after 28 days of continuous curing a trend of decline begins to occur.

Table 4.3: Compressive Strength Values of Plain CAC and CAC Blend Mixes Cured at 40°C (MPa)

|     | 1 day | 3 days | 7 days | 14 days | 28 days | 56 days | 90 days | 180 days |
|-----|-------|--------|--------|---------|---------|---------|---------|----------|
| C   | 33.3  | 22.0   | 24.0   | 22.6    | 26.4    | 27.3    | 31.8    | 27.6     |
| S20 | 28.9  | 21.0   | 26.4   | 32.9    | 32.8    | 37.8    | 41.4    | 47.6     |
| S40 | 19.3  | 18.6   | 25.5   | 29.7    | 29.9    | 29.9    | 31.1    | 32.9     |
| S60 | 9.6   | 11.7   | 14.4   | 16.0    | 15.3    | 15.7    | 15.9    | 17.4     |
| F10 | 30.4  | 20.2   | 17.9   | 21.9    | 25.6    | 28.4    | 34.0    | 39.7     |
| F20 | 25.5  | 19.0   | 15.3   | 19.6    | 23.3    | 24.4    | 30.9    | 33.5     |
| F30 | 21.1  | 15.3   | 11.6   | 15.9    | 19.0    | 21.5    | 24.6    | 27.6     |

Table 4.4: Compressive Strength Values of Plain CAC and CAC Blend Mixes Cured at 60°C (MPa)

|     | 1 day | 3 days | 7 days | 14 days | 28 days | 56 days | 90 days | 180 days |
|-----|-------|--------|--------|---------|---------|---------|---------|----------|
| C   | 25.1  | 25.0   | 26.1   | 25.8    | 25.4    | 25.9    | 27.2    | 30.2     |
| S20 | 22.7  | 23.8   | 24.2   | 23.4    | 24.8    | 24.9    | 25.0    | 38.0     |
| S40 | 14.9  | 14.2   | 17.3   | 24.7    | 15.8    | 16.2    | 15.4    | 26.7     |
| S60 | 7.8   | 9.7    | 11.6   | 8.4     | 14.6    | 14.2    | 14.8    | 15.6     |
| F10 | 23.8  | 23.5   | 24.5   | 25.4    | 27.7    | 32.1    | 33.5    | 36.5     |
| F20 | 18.0  | 16.1   | 20.4   | 20.5    | 21.2    | 22.6    | 24.2    | 31.4     |
| F30 | 14.5  | 11.7   | 15.8   | 16.9    | 14.8    | 16.3    | 21.6    | 23.4     |

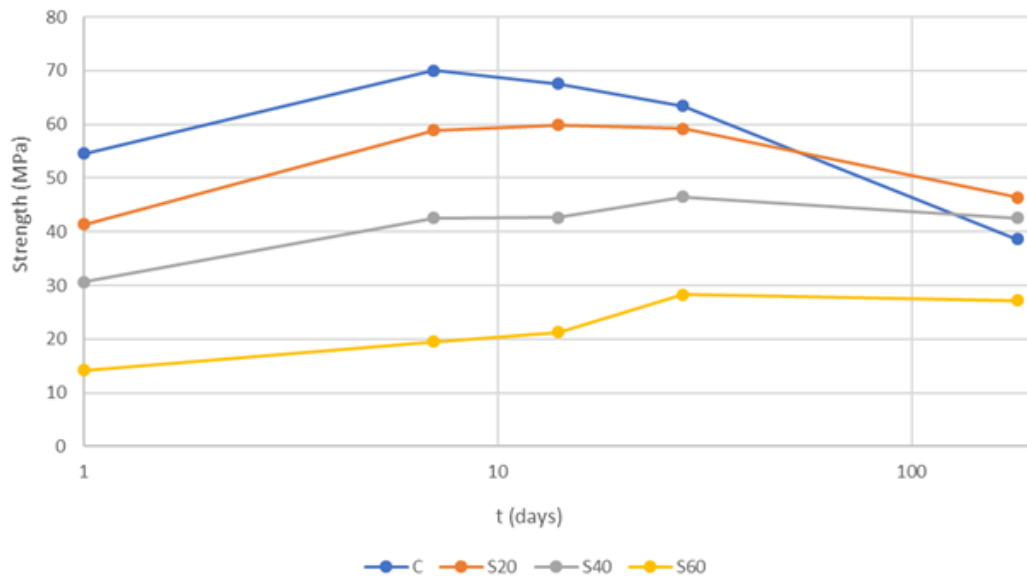


Figure 4.14: Age-strength relations for slag-incorporated CAC mortars in comparison with pure CAC mortars cured at 20°C

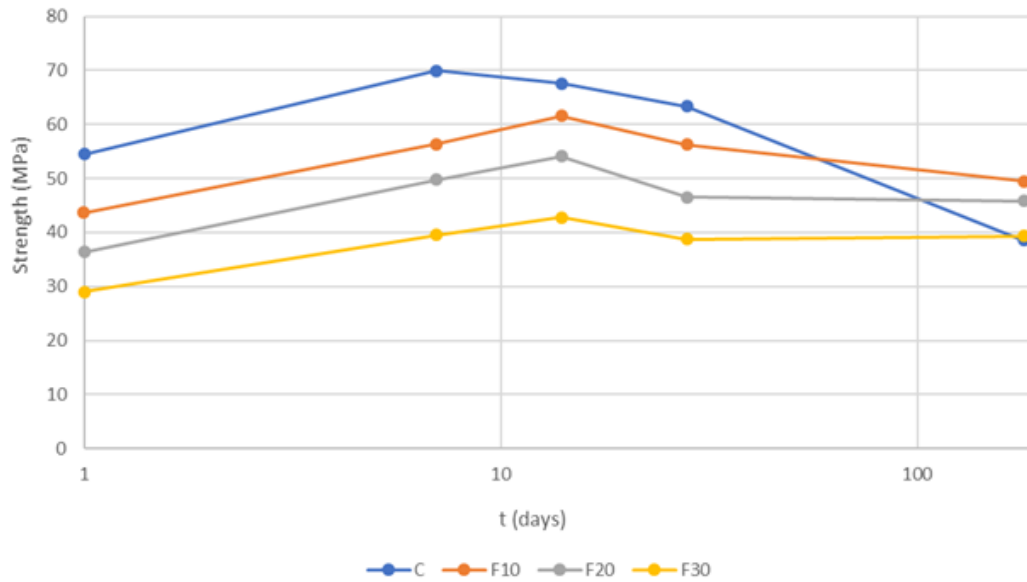


Figure 4.15: Age-strength relations for fly ash-incorporated CAC mortars in comparison with pure CAC mortars cured at 20°C

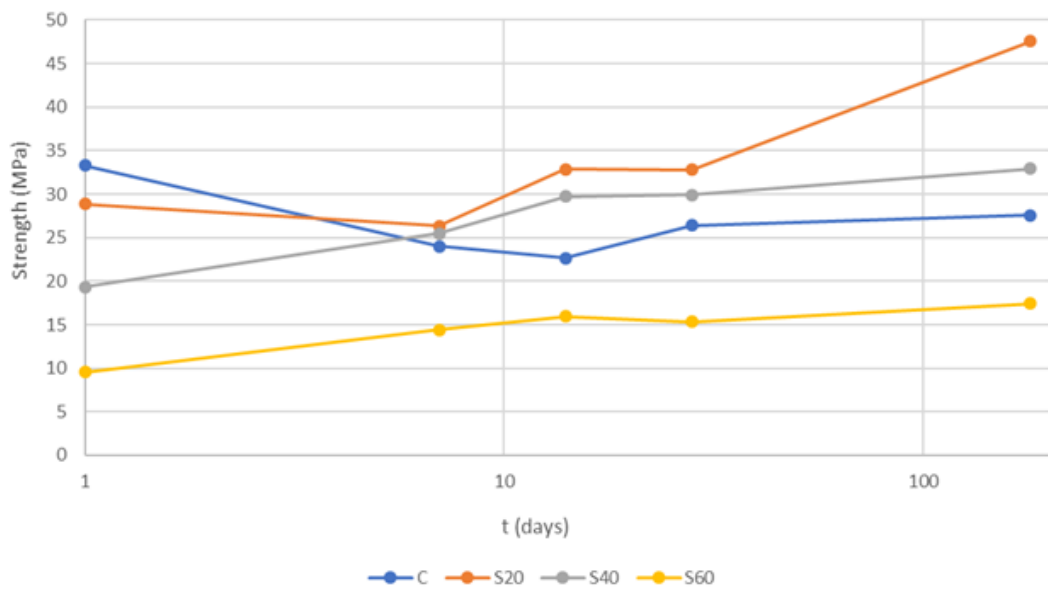


Figure 4.16: Age-strength relations for slag-incorporated CAC mortars in comparison with pure CAC mortars cured at 40°C

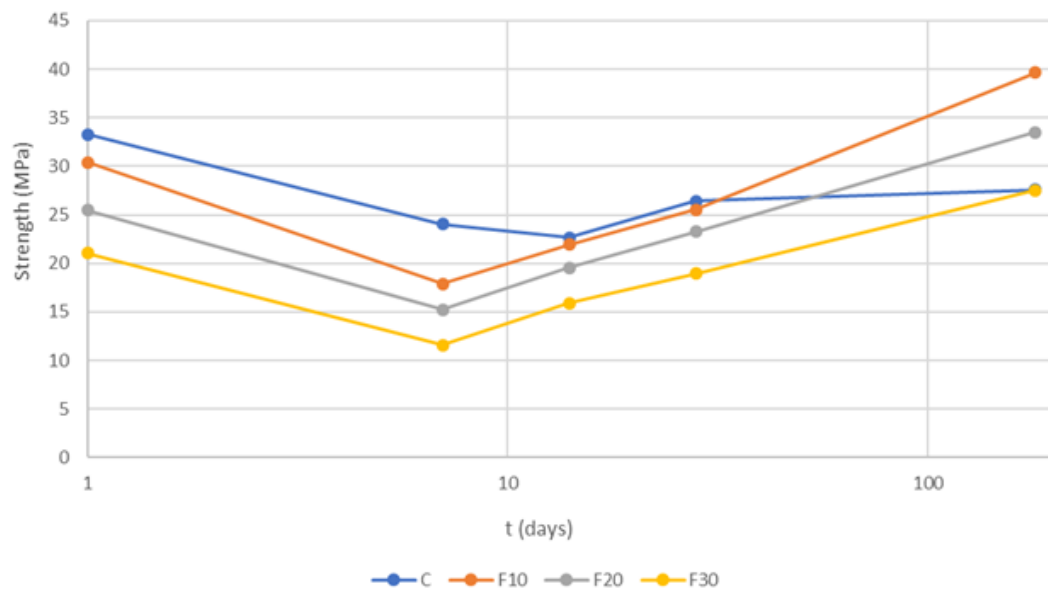


Figure 4.17: Age-strength relations for fly ash-incorporated CAC mortars in comparison with pure CAC mortars cured at 40°C

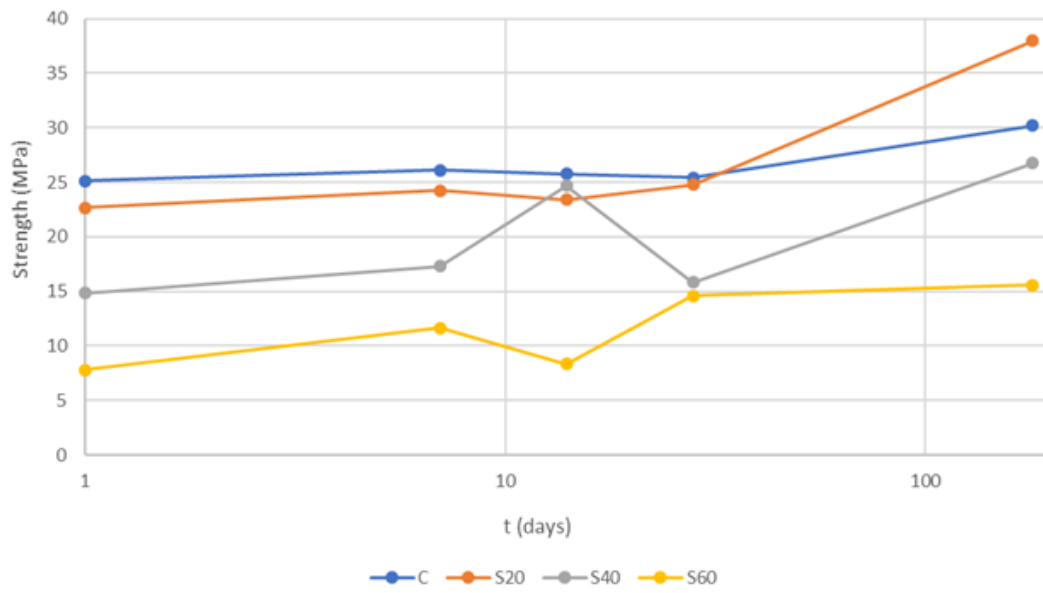


Figure 4.18: Age-strength relations for slag-incorporated CAC mortars in comparison with pure CAC mortars cured at 60°C

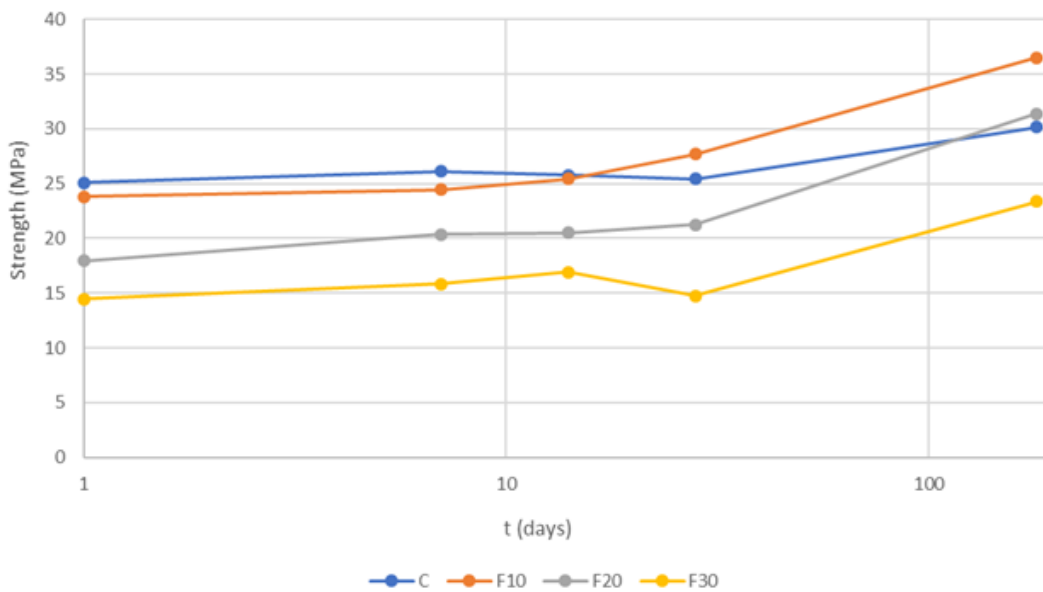


Figure 4.19: Age-strength relations for fly ash-incorporated CAC mortars in comparison with pure CAC mortars cured at 60°C

At the curing temperature of 20°C, the decreasing trend in the compressive strength test results for plain CAC corresponds to the age of 7 days therefore, the mix called S20 seems to postpone the commencement of the conversion period. On the contrary, mixes that contain 40 mass% and 60 mass% GGBFS have a compressive strength development which demonstrate an uninterrupted increase except for declines corresponding to 90th days of curing time. Despite the downcomes observed at the 90th days, a regain of compressive strength at the age of 180 days appears to be the case and reaches almost their maximum value throughout the entire period as well. The argument that 40 mass% and 60 mass% GGBFS incorporation into the plain CAC prevent the conversion from happening is emphasized in a significant amount of sources in the literature and the results obtained in this study also prove this case. [11,12,13] Yet the ultimate strength values taken into account, mixes named as S20 and S40 possess greater values than plain CAC does. Apart from all those, mixes containing fly ash mutually show a continuous rise in strength up to the age corresponding to 14 days and then a continuous decline after that point is seen likewise. Similarly, the strength values of plain CAC are greater than all CAC-FA blends up to that time nonetheless, at 180 days this case turns out to be total opposite as all CAC-FA blends have greater strength compared to neat CAC. On the other hand, when early strengths of blends are investigated, it can be stated that 1-day strength of CAC mortars is almost completely dependent on the formation of  $CAH_{10}$ , upon hydration. Slag- or fly ash-incorporation results in reduction in 1-day strength proportional with the amount of slag or fly ash used to partially replace CAC as shown in Figure 4.20.

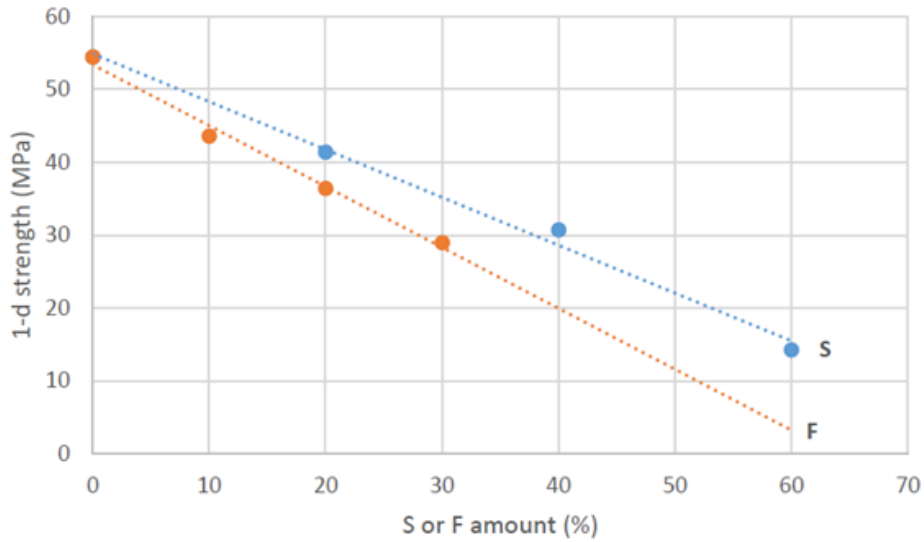


Figure 4.20: Effect of slag(S) or fly ash(F) incorporation on 1 day strength at 20°C

Since at this early age of 1 day, neither a significant conversion of CAC hydrated phases nor a chemical interaction between slag or fly ash and CAC occurs at 20°C, as can be justified in the XRD traces in Figure 4.21, the reduction in 1-day strength can only be attributed to the amount of slag or fly ash used to partially replace CAC.

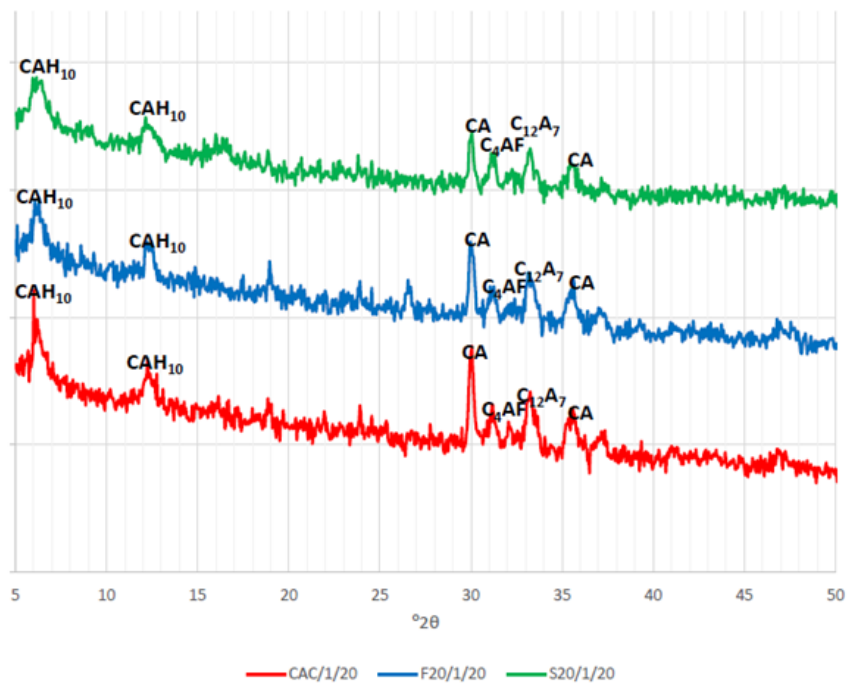


Figure 4.21: XRD traces of CAC and S- and F-incorporated pastes hydrated for 1 day at 20°C



It is clearly seen from Figures 4.14 and 4.15 that strength reduction in time is much less in slag and fly ash containing mortars although their early strengths are comparatively lower than that of the control CAC mortar. However, a satisfactory explanation of this behavior through XRD analyses is not possible. In other words, at 20°C, the major hydration product remained to be  $CAH_{10}$  at later ages and there was no evidence that there occurred a conversion into  $C_3AH_6$  as shown in Figure 4.22. Although it is claimed that CAC reacts with siliceous matter to result in straetlingite ( $C_2ASH_8$ ) formation, this reaction product was not detected in the X-ray diffractograms even at 180 days.

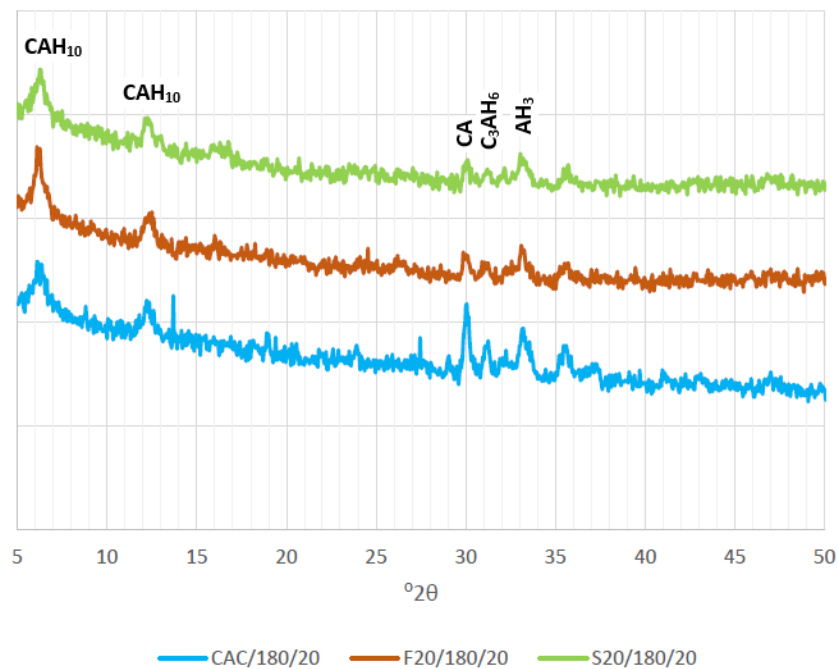


Figure 4.22: XRD traces of CAC and S- and F-incorporated pastes hydrated for 180 days at 20°C

Nevertheless, unlike pure CAC, later age strengths even after 180 days do not fall below those in 1 day, as illustrated in Figure 4.23. Therefore, it can be stated that use of GGBFS or fly ash as partial replacement of CAC is beneficial in preventing the strength loss through a physical, pore-filling effect at 20°C.

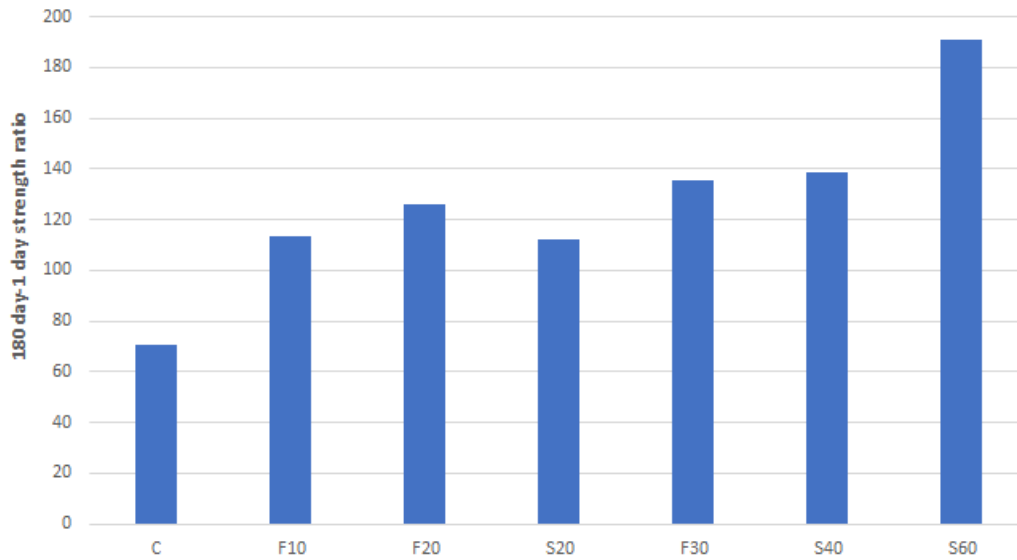


Figure 4.23: 180 days to 1 day strength ratios of mortars cured at 20°C

Consideration paid to the early strengths of blends cured at 40°C, it can be deduced that 1-day strength of CAC mortars is heavily dependent on the formation of  $C_2AH_8$  similar to the statements discussed for the curing temperature of 20°C. Either mineral admixture incorporation causes decrease in 1-day strength in proportion to the amount of mineral admixture incorporated. This effect can be seen by referring to Figure 4.24. When microstructures of GGBFS or fly ash blended mixes cured at 40°C at an age of 1 day are delved into, almost the same effect seem to be created by each of them. The formation of  $C_2AH_8$ ,  $C_3AH_6$  and  $C_2ASH_8$  exist at the same time. Thus, the strength of these mortars are related to the intensities of these phases. The microstructures mentioned above are illustrated in Figure 4.25. Among the GGBFS incorporated mixes cured at 40°C, S20 shows a drop in strength values at 3 days just like the decrease in plain CAC however, after 3 days a continuous strength gain observed to be the case. Even though a clear strength gain is not monitored for the strength development rate of neat CAC, an increment of approximately 65% can be seen when the 24-hour strength of S20 compared to the value at 180 days. If 180 days to 1 day strength ratios of all mortars cured at 40°C are compared, it is obvious that all mineral admixture incorporated mortars possess higher ratios as opposed to neat CAC mortars as shown in Figure 4.26. Based on Figure 4.26, it can also be

seen that mortars labelled as S60 gain around 80% strength when hydrated for 180 days compared to their initial 1 day strength value. On the other hand, strength gain ratios on the same time intervals are approximately 30% for all fly ash-incorporated mixtures regardless of their replacement ratios. Although in both 1 day hydrated and 180 day hydrated samples' X-Ray diffraction data indicate similar amounts of stable hydrates in fly ash and GGBFS incorporation, GGBFS-incorporated mixtures seem to gain more strength in the long-term period. Apart from these, S40 and S60 mixes have a constantly increasing strength gain rate just as the outcome obtained under 20°C moist curing. Therefore, GGBFS incorporation at the curing temperature of 40°C works quite effective in terms of obtaining both a constantly increasing strength trend and enhanced later age strength values. Further, a common point for all fly ash containing mixes to note is that they have relatively low early strength values however, after 7 days there is an increase seems to be appearing. Similar to the case with GGBFS addition, fly ash incorporation also results in higher ultimate strength values acquired at 180 days. As can be seen from Figure 4.17, fly ash incorporated mixes have the same or higher value than that of plain CAC.

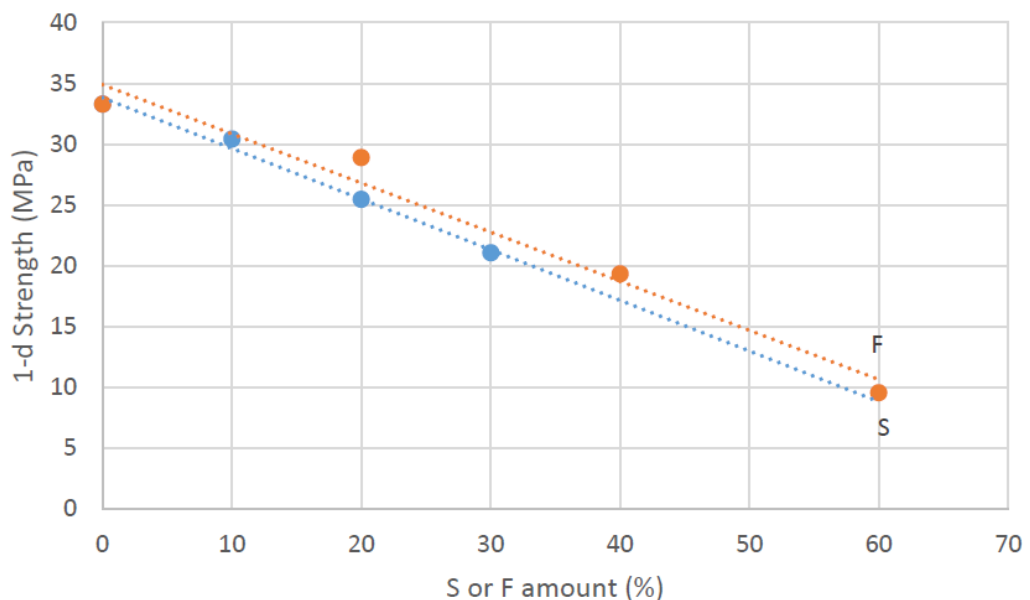


Figure 4.24: Effect of slag(S) or fly ash(F) incorporation on 1-day strength at 40°C

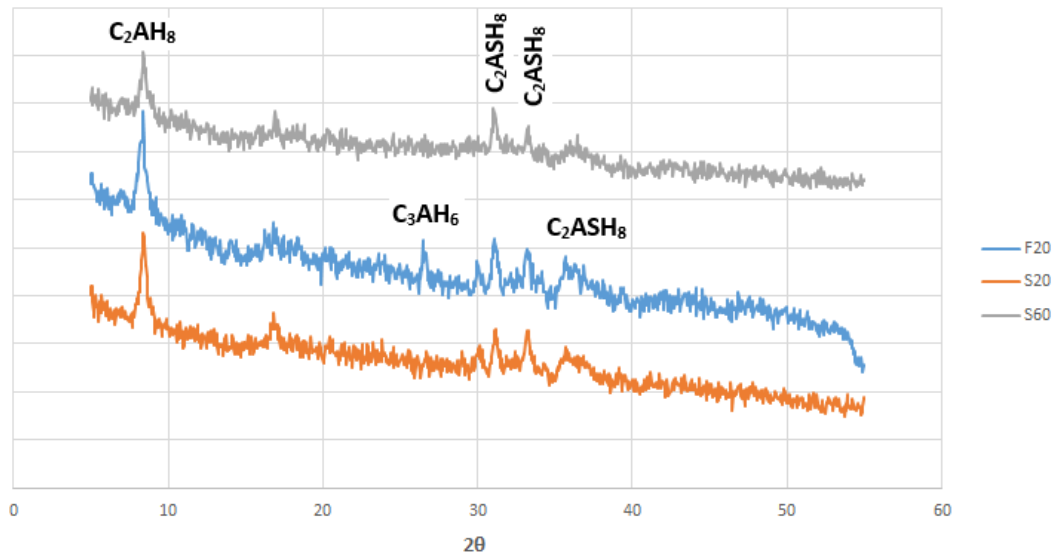


Figure 4.25: XRD traces of GGBFS and fly ash incorporated pastes hydrated for 1 day at 40°C

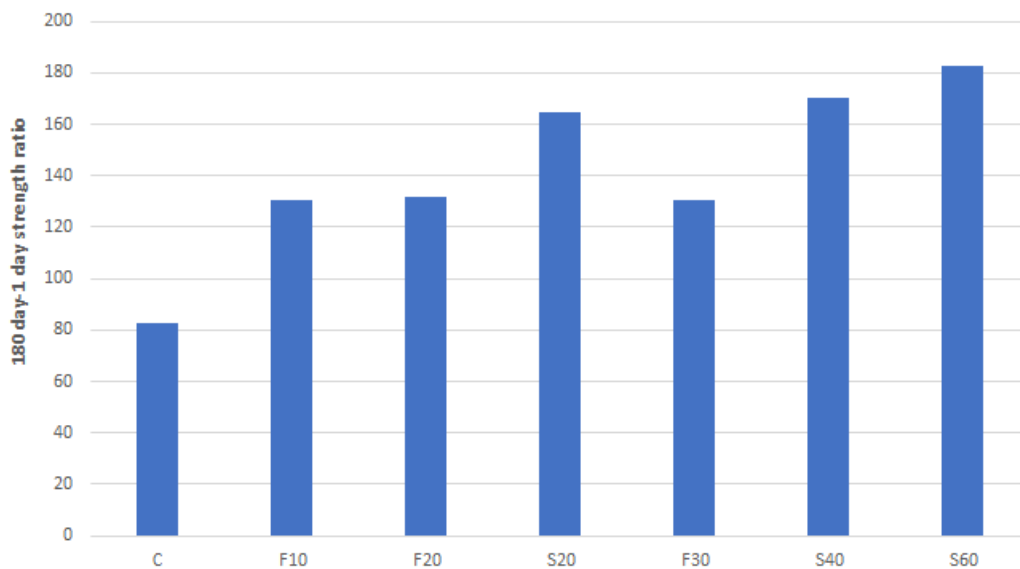


Figure 4.26: 180 days to 1 day strength ratios of mortars cured at 40°C

The fact that no clear conversion for neat CAC pastes cured at 60°C exist was emphasized in plain CAC section. Thus, in parallel with that, there is not an obvious increase or decrease trend seen in GGBFS incorporated mixes. Seemingly, the hydration process develops rapidly for mineral admixture incorporated CACs cured at 60°C

and does not display a significant alteration in the long term just as the case for plain CAC. Therefore, it can be said that at 60°C, stable  $C_3AH_6$  forms straightly as a result of the swift hydration due to the high temperature and a strong straelingite formation was not quite possible. In this respect, 180 days to 1 day strength ratios of mortars cured at 60°C are presented in Figure 4.27 so as to see changes in the long term. In addition to these, fly ash involving mixes share a similar feature with GGBFS incorporated mixes however, among all those, the mix called F10 has a relatively smooth increasing trend and the strength values of it are clearly higher than plain CAC pastes starting from 28 days curing and later on.

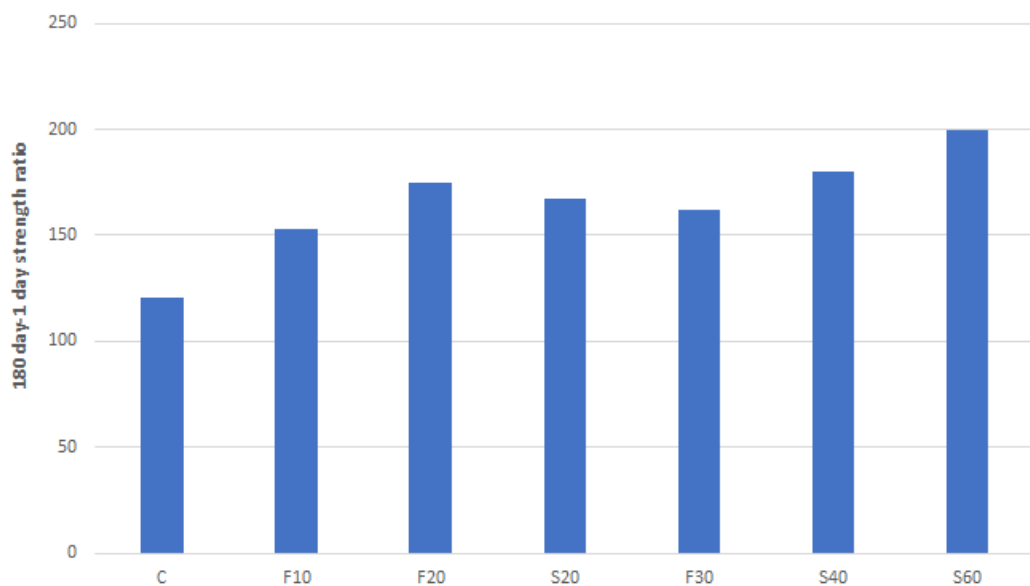


Figure 4.27: 180 days to 1 day strength ratios of mortars cured at 60°C

### 4.2.3 Effect on Microstructural Development

With the purpose of understanding what happens in the microstructural level that causes the compressive strength results stated in section 4.2.2, XRD studies were carried out at certain stages and the outcomes are presented in Figures 4.28 - 4.36.

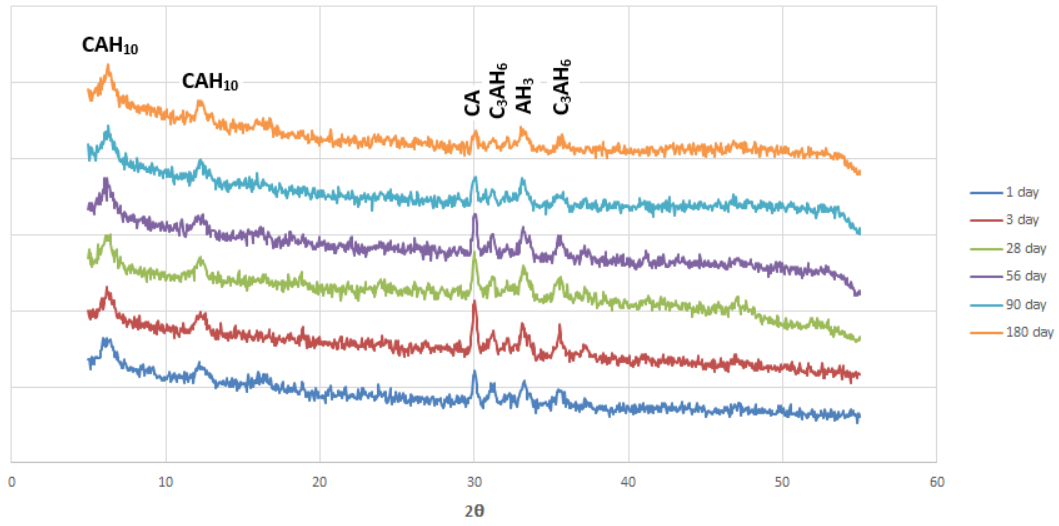


Figure 4.28: XRD Patterns of S20 Pastes cured at 20°C

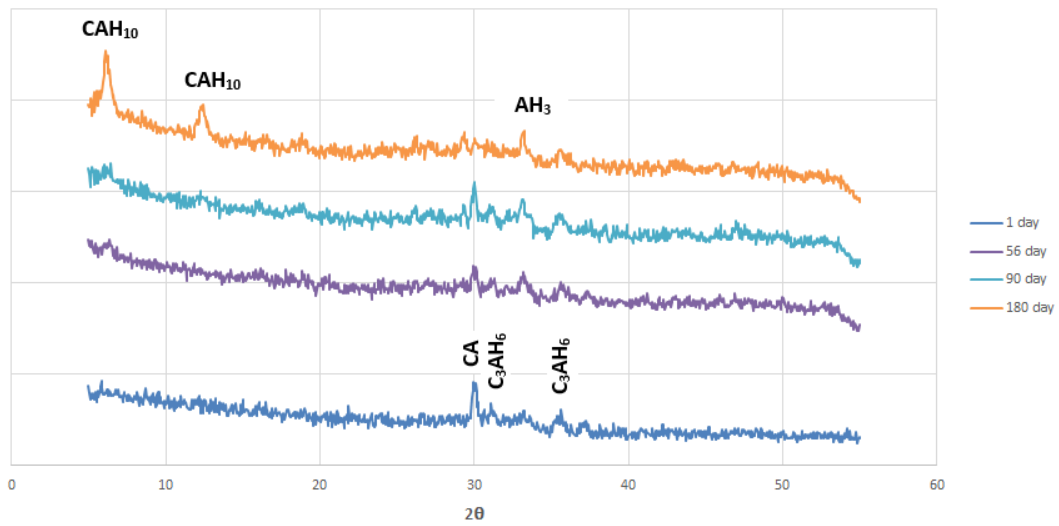


Figure 4.29: XRD Patterns of S60 Pastes cured at 20°C

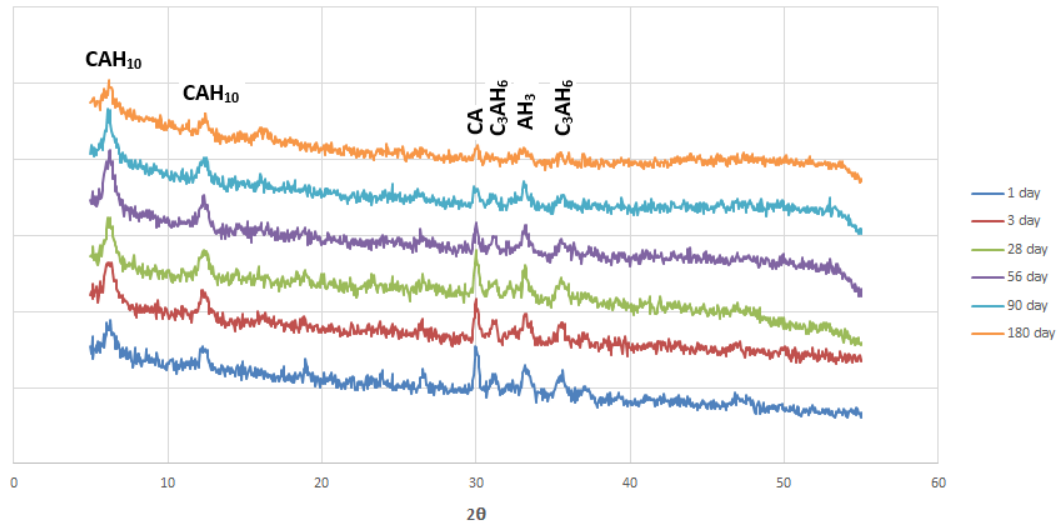


Figure 4.30: XRD Patterns of F20 Pastes cured at 20°C

XRD patterns of F20 and S20 mixes resemble each other and they show similar behaviour to the plain CAC pastes as well. This may be attributed to the straeltingite formation however, its formation is in a weak level which decreases the degree of conversion although not completely stops it. This is consistent with the compressive strength results as well where S20 and F20 mixes demonstrate a slight reduction but not as sharp as neat CAC pastes. For the S60 pastes, the straeltingite formation can be seen starting from the 1st day of curing and the peaks characteristic of it enhances at the later stages. Nevertheless, the straeltingite formation does not appear to be strong and this may be due to the fact that straeltingite are encapsulated by other hydrated phases. Another observation for the S60 pastes to note is at 180 days,  $CAH_{10}$  peaks are present and together with that clear peaks of  $C_3AH_6$  cannot be monitored at the same time. Therefore, one conclusion that may be derived from here is that either conversion was not really the case for these mixes or it happened quite slowly. To conclude it all, none of these three mixes whose hydration products were studied with the method of X-ray diffraction was able to stop the conversion completely at 20°C curing temperature.

The XRD diffraction patterns of mixes called S20, S60 and F20 that are cured at 40°C are presented in Figures 4.31, 4.32, 4.33 below.

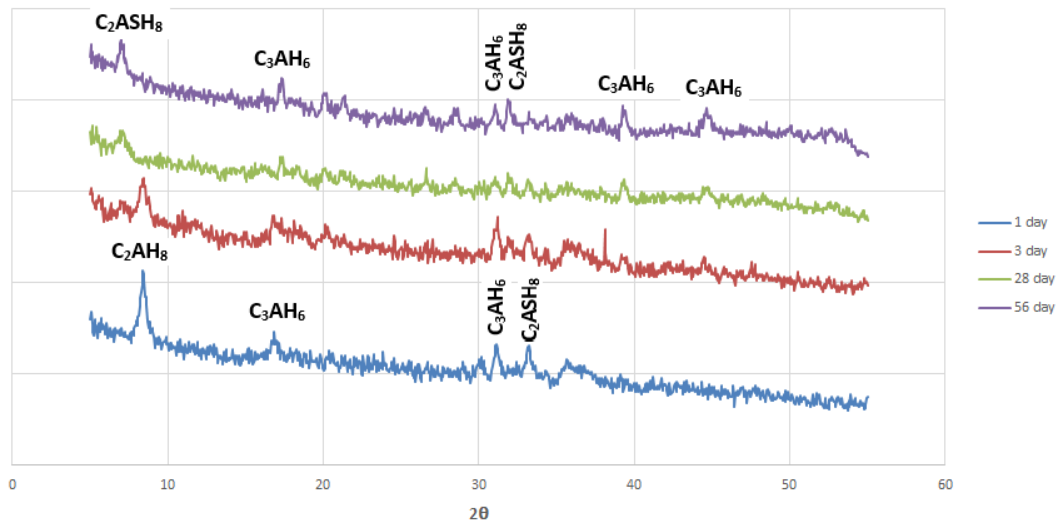


Figure 4.31: XRD Patterns of S20 Pastes cured at 40°C

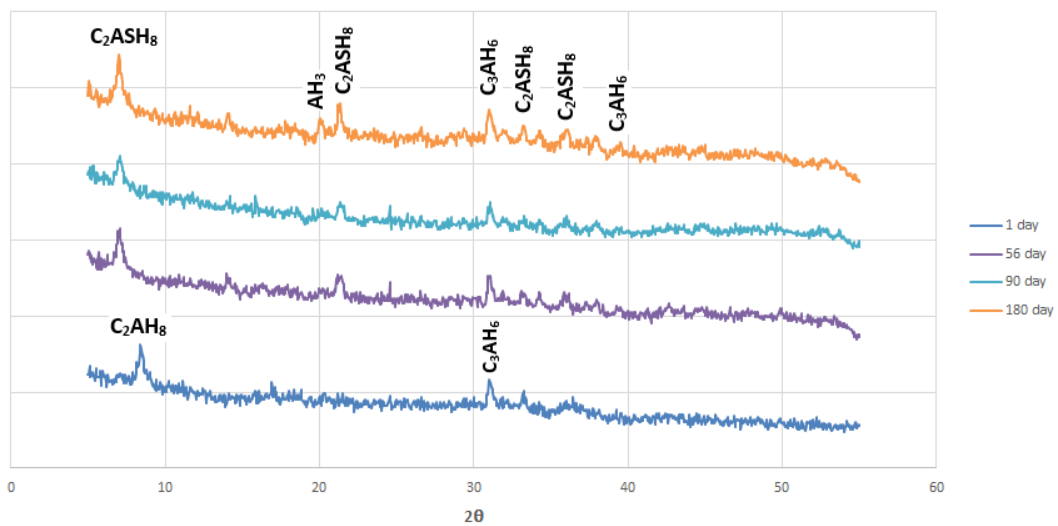


Figure 4.32: XRD Patterns of S60 Pastes cured at 40°C



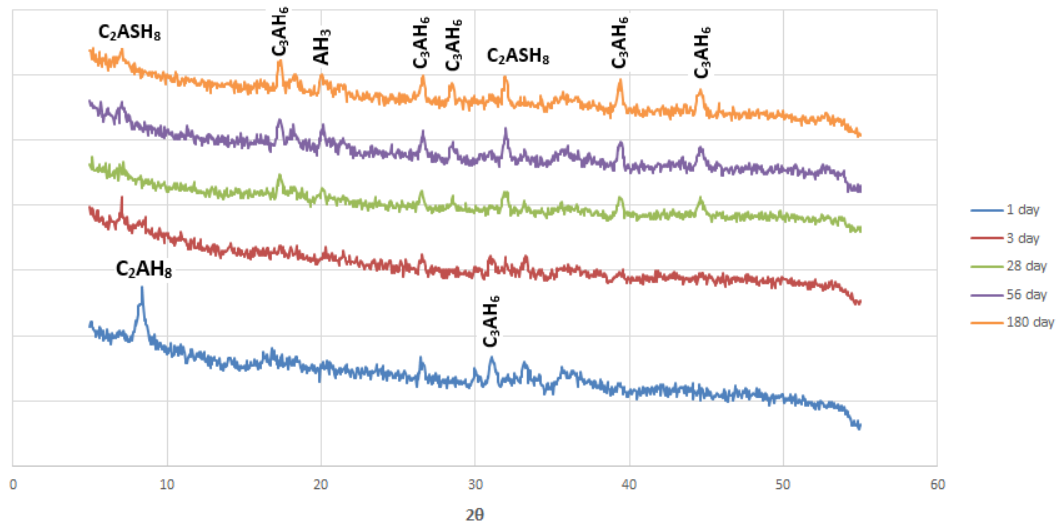


Figure 4.33: XRD Patterns of F20 Pastes cured at 40°C

From Figure 4.31, change in the phase formations appears to be quite clear.  $C_2AH_8$  formation seen in 1st day of curing still exist for 3 days, yet with a decline in the intensity of peak, and vanishes when the hydration progresses at 28 days and thereafter. At these later ages, stable products named  $C_3AH_6$  and straetlingite form thus, 20 mass% GGBFS replacement partially hinders conversion reactions as the formation of straetlingite as a gehlenite hydrate together with stable  $C_3AH_6$  can be seen at the same time. However, when it comes to S60 mix, straetlingite peaks develop in a much more clear fashion compared with the XRD pattern of S20. Even though there are tiny  $C_3AH_6$  and  $AH_3$  peaks that can be seen at different ages, straetlingite peaks outnumber them heavily. Consideration paid to the compressive strength development of these pastes, they show a steady rise during the whole curing period which can be explained by the strong formation of straetlingite peaks. By taking into account Figure 4.33, same statements given for S20 mixes may well be restated as they show similar behavior. Starting with the curing age 28 days,  $C_3AH_6$ ,  $AH_3$  and straetlingite formation coexist meanwhile, none of the unstable calcium hydrates, like  $CAH_{10}$  and  $C_2AH_8$ , appeared. The strength decrease caused by the conversion of  $C_2AH_8$  into  $C_3AH_6$  is compensated by the evolution of stable gehlenite hydrate straetlingite. To sum it all up, S20 and F20 mixes hinder the conversion to a certain degree whereas S60 was able to stop the conversion completely and these can be verified by a revision of strength results presented in section 4.2.2.

The XRD diffraction patterns of mixes called S20, S60 and F20 that are cured at 60°C are presented in Figures 4.34, 4.35, 4.36 below.

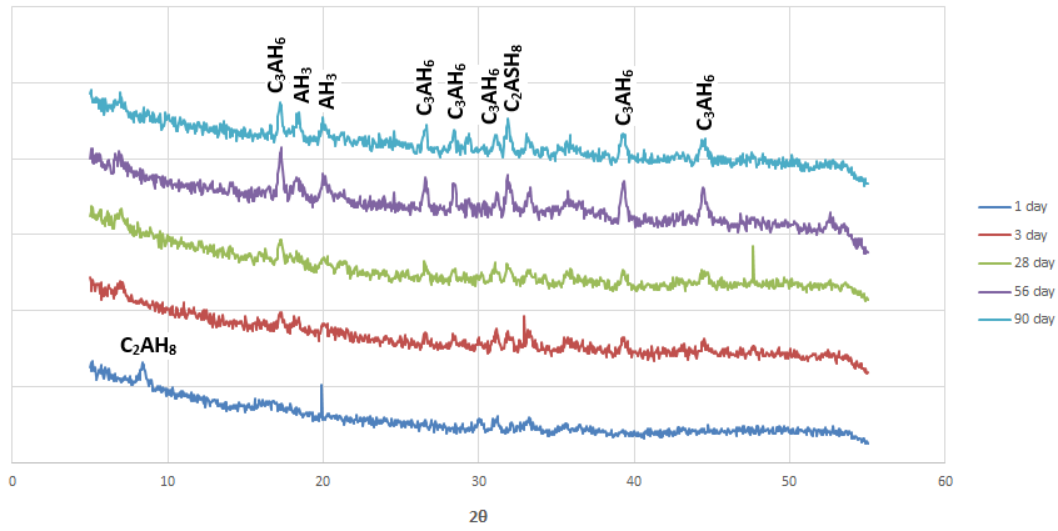


Figure 4.34: XRD Patterns of S20 Pastes cured at 60°C

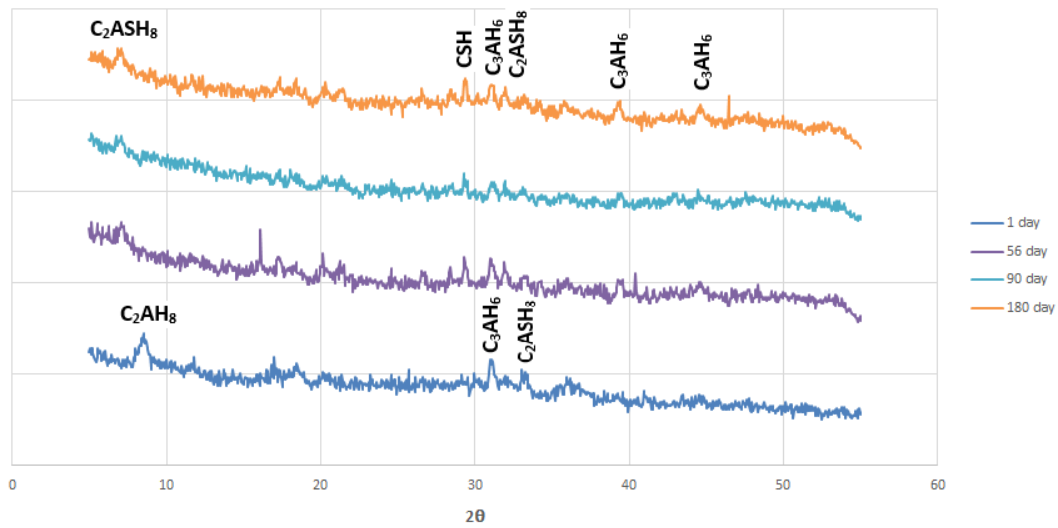


Figure 4.35: XRD Patterns of S60 Pastes cured at 60°C

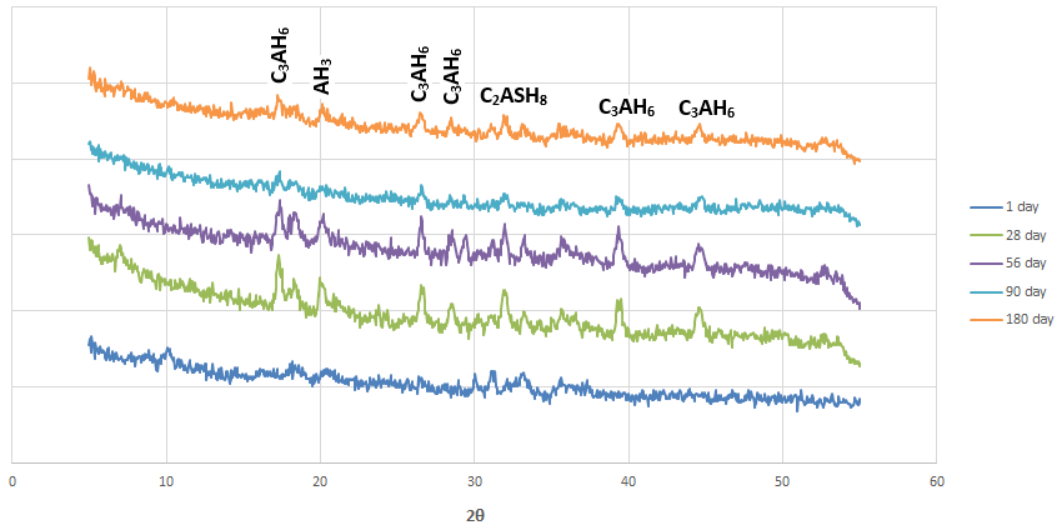


Figure 4.36: XRD Patterns of F20 Pastes cured at 60°C

The replacement of 20 mass% GGBFS does not seem enough to provoke the formation of straelingite in an adequate level as in Figure 4.34. Most of the unstable calcium aluminate hydrates seemingly converted into more stable ones which are  $C_3AH_6$  and  $AH_3$ . Reviewing the compressive strength development of the same mix, it can be distinguished that they have similar strength values with plain CAC pastes up to 90 days. As the XRD pattern shows this might be due to the similarity of hydration products or in other words, insufficient amount of straelingite present during the hydration stages of S20 mixes. In addition to that, weak straelingite peaks might be encapsulated by the large amount of  $AH_3$  gel originating as a consequence of conversion reactions. As opposed to the case explained for the mix S20, 60 mass% GGBFS replacement relatively provokes the straelingite development as unstable  $C_2ASH_8$  peak seen at first day disappears or more precisely, turns out to be  $C_3AH_6$ ,  $AH_3$  and mostly straelingite. This proves the case where strength development of S60 being on the rise particularly in comparison with other mixes. The same remarks addressed to the mix prepared with 20 mass% GGBFS mostly apply to the one involving 20 mass% fly ash. The unstable hydrates are exposed to the conversion quite swiftly due to the high temperature curing condition and that is why stable straelingite may not find the chance to reveal itself or in other words, a stable microstructure find it difficult to develop.



## CHAPTER 5

### CONCLUSIONS AND RECOMMENDATIONS

In this study, the effects of mineral admixture inclusion (blast furnace slag and fly ash) into CAC were examined. Compressive strength development and hydration process of CAC based mixtures were the focus throughout the examination. In light of the experimental results obtained in this study, the following conclusions can be reached:

- The rate of hydration reaction is highly temperature dependent. Elevated temperatures cause the reaction to happen more rapidly and particularly in this study, in rate of heat of hydration curves, it was observed that the dormant period observed at 20°C and 40°C hydrated specimens was not observed at 60°C due to the high rate of reaction.
- Since the fly ash is finer than the GGBFS used in this study, fly ash-incorporated mixtures have shortened dormant periods during hydration at a greater level compared with GGBFS incorporated mixtures.
- Among the plain CAC mortars cured at different temperatures, solely the one cured at 60°C seemed to gain strength over the testing period and this may be due to the swift progress of hydration so that stable  $C_3AH_6$  occurs immediately. Therefore, provoking the rapid formation of  $C_3AH_6$  through high temperature curing may be useful in terms of hindering long-term strength losses.
- Ultimate compressive strengths of neat CAC mortars corresponding to 180 days seem to revolve at similar values even though they were exposed to different curing temperatures and their early strengths were notably different.
- The high early strengths of plain CAC samples and the ones containing rel-

atively small amount of mineral admixture are attributed to the existence of metastable hydration products,  $CAH_{10}$  and  $C_2AH_8$ , as these products possess low densities and fill the pores. Their existence is proven with the X-Ray diffractograms.

- At elevated temperatures, direct formation of straelingite or formation through conversion is more obvious. At the curing mode of 20°C, the existence of metastable  $CAH_{10}$  and  $C_2AH_8$  still last as seen through X-Ray diffraction patterns.
- Compressive strength development of plain CAC at 40°C demonstrates a sharp decrease in strength at 3 days and this effect is less in slag-incorporated mixtures and the mixture containing 60 mass% slag continuously gain strength. This is due to the conversion of  $C_2AH_8$  into  $C_2ASH_8$  with the presence of amorphous silica coming from GGBFS. Fly ash-incorporated mixtures do not show such a strongly correlated behavior.
- One common conclusion regardless of curing temperature is that the mixtures containing 40 mass% slag showed hindered strength reductions at some certain levels however, the mixtures containing 60 mass% slag do not show strength loss, except for 20°C at later ages, and they almost doubled their 1 day strength value when they were left for curing up to 180 days at all temperatures. This result is consistent with the information given in literature and proves once again that using GGBFS is highly useful to obtain a continuously increasing strength trend.

The following recommendations could be used for future researches and studies:

- The fineness values of the cement replacement materials seem to have a decent effect on hydration behaviour and strength development of blended CAC-based mixtures. For this reason, the same cement replacement material possessing different fineness values may be tested simultaneously to observe the effect of fineness of pozzolanic materials on mineral admixture incorporated mixtures.
- Two different types of fly ashes one of them being low lime fly ash and the other being high lime fly ash can be used to prepare different blends so that seeing

the effect of lime content of fly ash on CAC based composite mixtures can be possible.

- Use of different mineral admixtures along with fly ash and GGBFS can also provide beneficial effects on the long-term performance of CAC blended mixtures thus, it can be useful to utilize the possible positive influence they can offer.
- The effect of chemical additives particularly water reducing agents and retarding agents worth investigating as they have the potential to create more workable mixtures potentially allowing the use of higher replacement ratios of mineral admixtures in CAC involving binders.
- In this study, the lowest curing temperature was decided to be 20°C which can be thought as standard ambient temperature. However, what may possibly occur in the strength development trends of CAC blends as well as their hydration behaviour at lower temperatures would be useful investigate.
- In this study, hydration properties of mineral admixture incorporated CACs were investigated for a 24 hour period. Nonetheless, the rate of heat evolution and total heat of hydration values of mixtures in the long term can give ideas about why these mixtures demonstrate strength losses at certain testing ages.
- In this study, mineral admixtures were used as cement replacement materials at certain replacement ratios. However, using mineral admixtures as additions rather than replacement has the potential to produce useful results thus, that kind of usage may be studied.
- All materials might suffer attacks due to the chemically aggressive environment they can be potentially in contact with. Even though CAC is reported to be fairly durable against chemically aggressive environment, testing mineral admixture incorporated CACs against such conditions may produce beneficial results which can lead a way to the use of such mineral admixtures together with commercially available CACs.





## REFERENCES

- [1] H.F.W. Taylor. *Cement Chemistry*. Thomas Telford, 1997.
- [2] Çimsa Çimento Araştırma ve Uygulama Merkezi. <https://www.cimsa.com.tr/ca/docs/4FE58AA58E3A4B7B85FA9E4EE011A8/4CB4AB8E1EB74220AB72D7B93589476E.pdf>. Last Accessed: 2018-07-10.
- [3] TS EN 14647. Calcium aluminate cement - Composition, specifications and conformity criteria. *Ankara: Turkish Standard Institution*, 2010.
- [4] K. L. Scrivener and A. Capmas. 13 - Calcium aluminate cements. In Peter C. Hewlett, editor, *Lea's Chemistry of Cement and Concrete (Fourth Edition)*, pages 713 – 782. Butterworth-Heinemann, Oxford, fourth edition edition, 1998.
- [5] O. López-Zaldívar, R.V. Lozano-Díez, A. Verdú-Vázquez, and N. Llauradó-Pérez. Effects of the addition of inertized msw fly ash on calcium aluminate cement mortars. *Construction and Building Materials*, 157:1106 – 1116, 2017.
- [6] M.C.G. Juenger, F. Winnefeld, J.L. Provis, and J.H. Ideker. Advances in alternative cementitious binders. *Cement and Concrete Research*, 41(12):1232 – 1243, 2011. Conferences Special: Cement Hydration Kinetics and Modeling, Quebec City, 2009.
- [7] K. Scrivener. 2 - Calcium aluminate cements. In John Newman and Ban Seng Choo, editors, *Advanced Concrete Technology*, pages 1 – 31. Butterworth-Heinemann, Oxford, 2003.
- [8] V. Antonovic, J. Keriene, R. Boris, and M. Aleknevičius. The effect of temperature on the formation of the hydrated calcium aluminate cement structure. *Procedia Engineering*, 57:99 – 106, 2013.
- [9] Ö. Kırca, İ. Ö. Yaman, and M. Tokyay. Compressive strength development of calcium aluminate cement–ggbf s blends. *Cement and Concrete Composites*, 35(1):163 – 170, 2013.
- [10] M. Heikal, M.S. Morsy, and M.M. Radwan. Electrical conductivity and phase composition of calcium aluminate cement containing air-cooled and water-cooled slag at 20, 40 and 60° C. *Cement and Concrete Research*, 35(7):1438 – 1446, 2005.

- [11] M. Heikal, M.M. Radwan, and O.K. Al-Duaij. Physico-mechanical characteristics and durability of calcium aluminate blended cement subject to different aggressive media. *Construction and Building Materials*, 78:379 – 385, 2015.
- [12] K. Quillin, G. Osborne, A. Majumdar, and B. Singh. Effects of w/c ratio and curing conditions on strength development in brecem concretes. *Cement and Concrete Research*, 31(4):627 – 632, 2001.
- [13] B. Singh, A.J. Majumdar, and K. Quillin. Properties of BRECEM: Ten-year results. *Cement and Concrete Research*, 29(3):429 – 433, 1999.
- [14] B. Pacewska, I. Wilińska, and M. Nowacka. Studies on the influence of different fly ashes and portland cement on early hydration of calcium aluminate cement. *Journal of Thermal Analysis and Calorimetry*, 106(3):859–868, 2011.
- [15] M. Collepari, S. Monosi, and P. Piccioli. The influence of pozzolanic materials on the mechanical stability of aluminous cement. *Cement and Concrete Research*, 25(5):961 – 968, 1995.
- [16] R. Barborak. Calcium aluminate cement concrete (class cac concrete) txdot special specification ss-4491 tip sheet. *Texas Department of Transportation, Austin, TX*, 2010.
- [17] I. Odler. *Special Inorganic Cements*. Modern Concrete Technology. Taylor & Francis, 2003.
- [18] B. Pacewska, M. Nowacka, M. Aleknevičius, and V. Antonovič. Early hydration of calcium aluminate cement blended with spent fcc catalyst at two temperatures. *Procedia Engineering*, 57:844 – 850, 2013.
- [19] E.T. Carlson. Some observations on hydrated monocalcium aluminate and monostrontium aluminate. *Journal of Research of the National Bureau of Standards*, 59(2):107, 1957.
- [20] J.W. Anthony. *Handbook of Mineralogy*. Number 2. c. in Handbook of Mineralogy. Mineral Data Publishing, 1995.
- [21] T.D. Robson. *High-alumina cements and concretes*. Concrete library. Contractors Record, 1962.
- [22] H. Eldidamony, A.M. Sharara, I.M. Helmy, and S. El-Awey. Hydration characteristics of Beta-C2S in the presence of some accelerators. *Cement and Concrete Research*, pages 1179–1187, 1996.
- [23] TS EN 197-1. Cement-Part 1: Composition, specifications and conformity criteria for common cements. *Ankara: Turkish Standard Institution*, 2012.

- [24] J.I Escalante-Garcia and J.H Sharp. The microstructure and mechanical properties of blended cements hydrated at various temperatures. *Cement and Concrete Research*, 31(5):695 – 702, 2001.
- [25] N. Y. Mostafa, Z.I. Zaki, and O. H. Abd-Elkader. Chemical activation of calcium aluminate cement composites cured at elevated temperature. *Cement and Concrete Composites*, 34(10):1187 – 1193, 2012.
- [26] Ö. Kirca. Temperature effect on calcium aluminate cement based composite binders. *Ankara: Middle East Technical University*, 2006.
- [27] ASTM C204. Standard test method for fineness of hydraulic cement by air permeability apparatus, 2000.
- [28] R. A. Sanderson, G. M. Cann, and J. L. Provis. Comparison of calorimetric methods for the assessment of slag cement hydration. *Advances in Applied Ceramics*, 116(4):186–192, 2017.
- [29] TAM Air Calorimeter Operator’s Manual. *U.S.A: TA Instruments*, 2007.
- [30] T. Degen, M. Sadki, E. Bron, U. König, and G. Nénert. The highscore suite. *Powder Diffraction*, 29(1):13–18, 2014.
- [31] TS EN 196-1. Methods of testing cement-Part 1: Determination of strength. *Ankara: Turkish Standard Institution*, 2016.
- [32] N. Ukrainczyk and T. Matusinović. Thermal properties of hydrating calcium aluminate cement pastes. *Cement and Concrete Research*, 40(1):128–136, 2010.
- [33] L. Xu, K. Wu, C. Rößler, P. Wang, and H.M. Ludwig. Influence of curing temperatures on the hydration of calcium aluminate cement/portland cement/-calcium sulfate blends. *Cement and Concrete Composites*, 80:298–306, 2017.
- [34] T. Matusinović, J. Šipušić, and N. Vrbos. Porosity–strength relation in calcium aluminate cement pastes. *Cement and Concrete Research*, 33(11):1801 – 1806, 2003.
- [35] C. Bradbury, P.M. Callaway, and D.D. Double. The conversion of high alumina cement/concrete. *Materials Science and Engineering*, 23(1):43–53, 1976.